CHALMERS
UNIVERSITY OF TECHNOLOGY

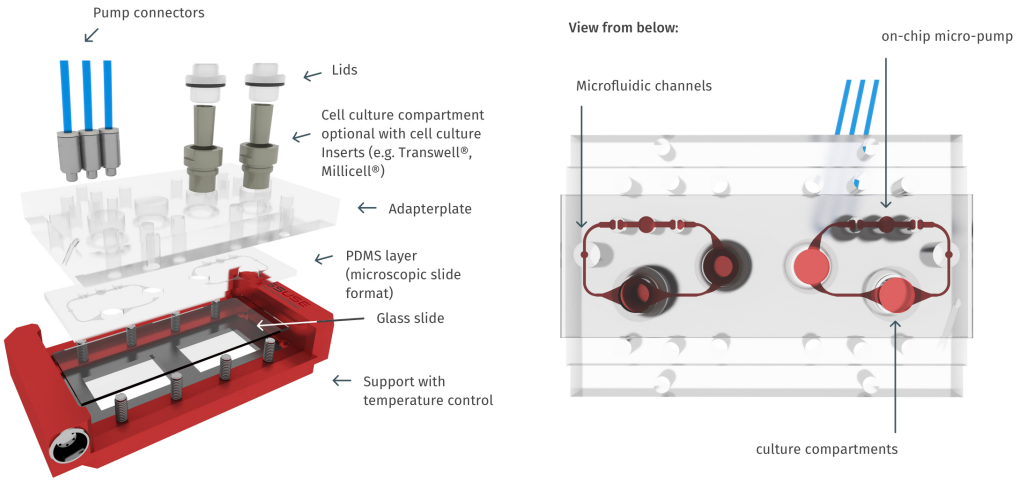

Human liver spheroid cultures in microfluidic chip co-cultures and comparative MetID studies

Master of Science Thesis in Biotechnology

JOHANNA ASSERLIND

Department of Physics
CHALMERS UNIVERSITY OF TECHNOLOGY
Gothenburg, Sweden 2017

Master's thesis 2017

Human liver spheroid cultures in microfluidic chip co-cultures and comparative MetID studies

Johanna Asserlind

CHALMERS
UNIVERSITY OF TECHNOLOGY

Department of Physics
Division of Biological Physics
Chalmers University of Technology
Gothenburg, Sweden 2017

Human Liver Spheroid Cultures in Microfluidic Chip Co-cultures and Comparative MetID Studies

Johanna Asserlind

Supervisor: Kajsa Kanebratt, AstraZeneca, Mölndal
Examiner: Julie Gold, Department of Physics

Master's Thesis 2017
Department of Physics
Division of Biological Physics
Chalmers University of Technology
SE-412 96 Gothenburg

Cover: Schematic figure of the 2-organ-chip used for this thesis, courtesy of TissUse GmbH.

Printed by Chalmers Reproservice
Gothenburg, Sweden 2017

Abstract

The liver is the most important site of drug metabolism in the human body. During drug development, it is therefore of high importance to employ a robust *in vitro* model that resembles the *in vivo* microenvironment, and is able to accurately predict the metabolism and disposition of compounds. This thesis is divided into two major parts. First, the metabolism of a set of compounds was characterized qualitatively in spheroids made from primary human hepatocytes (PHH), and the resulting data was compared to previous data from hepatocyte suspension culture and human *in vivo* data. The metabolites formed during a 72 hour incubation period was analyzed by LC-MS. Second, a co-culture between human liver spheroids, made from HepaRG cells and primary hepatic stellate cells, and primary human pancreatic islets in microfluidic 2-organ-chips was established, and the liver spheroids were functionally characterized. A total of 5 chip experiments were performed, where each chip experiment lasted for 7 days, and different conditions such as medium composition where examined. Various staining techniques and measurements of secreted albumin and LDH were used to assess long-term sustainability, function and viability of the spheroids.

Some of the metabolites seen in humans were also formed in PHH spheroids, but the spheroid model was not able to fully predict the human *in vivo* metabolism. Spheroids were not shown to be a significantly better model to use compared to suspension cultures during these experiments. CYP activity analysis showed that decreasing metabolic function after a change in medium composition might be a factor. HepaRG spheroids were able to display several liver-like functions when cultured in the multi-organ chips, but the large size of the spheroids led to the formation of necrotic cores. Overall, while certain parameters need to be improved, the liver spheroids are promising models for studying several different aspects of liver functions as well as for establishing organ system models.

Keywords: Liver, 3D *in vitro* model, spheroids, HepaRG, primary human hepatocytes, stellate cells, co-culture, MetID, microfluidics, organs-on-chips

Acknowledgements

First, I would like to thank my supervisor Kajsa Kanebratt and Tommy B. Andersson for presenting me with this opportunity of doing my master's thesis at Astra Zeneca within this relatively new and intriguing field of research, and for all the unending help and guidance, feedback and useful input I needed on my way.

Special thanks to

Martin Hayes for his immense effort to help me run all LC/MS samples, as well as analyze, understand and compile the resulting data.

Charlotte Wennberg Huldt for her assistance with the multi-organ chips and helping me with the ELISA assay.

Karin Jennbacken for answering all my questions regarding immunofluorescent staining and optimizing the staining protocol.

Gerhard Böttcher for his useful input on the H&E and PAS stainings of the spheroids.

Emre Isin for the private lecture regarding hepatic metabolism and the beneficial discussions around the MetID project.

A massive thanks to Matthew O'Hara for patiently answering all my questions and guiding me through most assays and analyses used in this thesis.

My thanks also goes out to all the people in the CVMD DMPK department at Astra Zeneca, for letting me be part of your department for a full year, and my supportive friends and family.

Johanna Asserlind, Gothenburg, June 2017

Contents

ADME Absorption, Distribution, Metabolism and Elimination
ACN Acetonitrile
BSA Bovine Serum Albumin
CYP Cytochrome P450
ECM Extracellular Matrix
ELISA Enzyme-linked Immunosorbent Assay
FA Formic Acid
FBS Fetal Bovine Serum
H&E Hematoxylin & Eosin
HSGM Human Hepatic Stellate Cell Growth Medium
ICC Immunocytochemistry
IHC Immunohistochemistry
ITS Insulin-Transferrin-Selenium
LC Liquid Chromatography
LDH Lactate Dehydrogenase
MetID Metabolite Identification
MOC Multi-organ Chip
MS Mass Spectrometry
PAS Periodic Acid-Schiff Stain
PBS Phosphate Buffered Saline
PDMS Polydimethylsiloxane
PHH Primary Human Hepatocytes
PLL Poly-L-lysine
SMA Smooth Muscle Actin
SteC Stellate Cells
ULA Ultra-low Attachment
WME William's Medium E

1. Introduction

The process of developing new drugs is highly expensive and time-consuming, and only a few substances are taken through all the phases of the lengthy development procedure. To help ensure human safety and the efficacy of drug candidates, new pharmaceuticals are often tested *in vitro* or in animals. However, the *in vitro* systems currently used often fail to imitate the intrinsic organ complexity of the human body and thereby fail to predict the effects of new drugs in humans. Even experiments performed *in vivo* are not fully reliable, since the phylogenetic distance between humans and laboratory animals is too large [1]. It is therefore of high importance to develop new technologies to overcome these discrepancies and limitations.

1.1 Background

The human body is exposed to a variety of chemicals each day, of which many can be extremely toxic. The primary defense mechanism in the body against these xenobiotics are the drug metabolizing enzymes present in the liver [2][3]. The liver is an immensely complex organ capable of performing numerous functions in the body, including protein synthesis and secretion, nutrient metabolism, and detoxification of xenobiotics. It is made from several different cell types with different phenotypes and functions highly dependent on their physical location and coordination within the intricate tissue architecture [2]. Understanding and studying the biology and functions of the liver is therefore a difficult task.

Because the liver is the most important site of drug metabolism, several *in vitro* models, mimicking key aspects of the *in vivo* biotransformation of the human liver, have been developed. In order to assess drug uptake and metabolism, enzyme induction, and drug interactions possibly affecting metabolism and hepatotoxicity, these *in vitro* models are used during drug development. By screening lead candidates in *in vitro* models of the liver, nearly all potentially harmful compounds are identified and rejected. In fact, almost 90% of all lead candidates fail to proceed to clinical trials after screening through liver *in vitro* models [4]. However, of those that do continue on to Phase I clinical trails, more than 50% fail during clinical trials due to unforeseen human liver toxicity or bioavailability issues [4][5]. There is therefore an urgent need for improved methods to predict human liver metabolism of drugs already at an *in vitro* stage.

The main issue lies within the most common models used. As mentioned above, results from animal testing cannot be fully extrapolated to humans. These types of experiments are also expensive, lengthy and subject to ethical issues [6]. The most commonly used *in vitro* models are either suspension or 2D cell culture models using hepatocytes, which fail to recreate the *in vivo* cellular microenvironment and are unable to maintain their differentiated functions [7]. In order to overcome these limitations, 3D cell culture models were developed. This approach improves tissue organization, enhancing natural cell-cell and cell-matrix interactions, and improves the maintenance of differentiated functions [7][8].

One such cell culture model that has received a lot of attention lately is the liver spheroid model. These have been shown to behave more natively compared to cells in 2D or suspension cultures [9]. They are also able to maintain their viability and functions for weeks in culture and have been extensively characterized [8].

Nevertheless, 3D culture systems also have certain restraints. For instance, many systems lack tissue-tissue interfaces and signaling, as well as mechanical cues such as fluid shear stress, which influence cell differentiation and function *in vivo*. Culturing cells on microfluidic devices offers a possibility to overcome these limations [7][10]. These systems combine human microtissues in an organ-like arrangement at a homeostatic steady state. Previously generated multi-channel 3D microfludic cell culture systems are able to support the molecular interplay between different tissue culture compartments through media re-circulation [11]. The advantage of using such a system is the ability to adjust the fluid flow to provide proper dynamic mechanical and chemical signals to the microtissues, as well as the ability to control the local tissue-to-fluid ratios, imitating the *in vivo* microenvironment.

A multi-organ chip was recently developed by TissUse GmbH and the Technical University of Berlin with an integrated peristaltic micropump and separate culture compartments interconnected with microfluidic channels, minimizing the fluid-to-tissue ratio within the system [12]. This setup provides a more lifelike behavior and ensures crosstalk between the integrated tissues. The system supports co-cultures of three-dimensional organ equivalents $^{1}/_{100000}$ of the biomass *in vivo*, and has been shown to maintain the functionality and viability of the organoids for up to 28 days, as well as inducing substance sensitivity different from single-tissue cultures due to the enhanced cross-talk between tissues [12][13][14][15]. There are two types of chips available, capable of co-culturing either two or four organ equivalents, of which the two-organ-chip has been used for this thesis. They are highly suitable for microfluidic administration, distribution, metabolism and excretion (ADME) studies, as well as systemic toxicity analysis. These microfluidic systems also offer a unique possibility to create and study miniaturized human disease models, and convey a significant step towards creating a human-on-a-chip [10][14].

1.2 Aim

This project is divided into two major parts. The aim of the first part was to characterize the metabolites formed in spheroids made from primary human hepatocytes from a set of compounds, and evaluate whether they are able to sufficiently predict the *in vivo* metabolism in humans compared to hepatocyte suspension cultures. The set of compounds for these experiments was selected based on a previous report, for which there is already *in vitro* (hepatocyte suspension) data, as well as human *in vivo* data available [16]. Spheroids were incubated with the selected compounds for a total of 72 hours. The supernatant and the cells were sampled at 0, 4, 8, 24, 48, and 72 hours after addition of the compounds and the samples were analyzed via mass spectrometry. The functionality of the main drug metabolizing enzymes in spheroids was assessed by characterizing the activity of 4 cytochrome P450s.

The second component of this thesis is part of a larger ongoing project at AstraZeneca. The aim of this part was to establish and characterize a co-culture between human liver spheroids, made from HepaRG cells and primary hepatic stellate cells, and primary hu-

man pancreatic islets in microfluidic 2-organ-chips. Liver spheroids were manufactured from freshly thawed cryopreserved cells, or pre-cultured cryopreserved cells. Spheroids and pancreatic islets were co-cultured in separate compartments for 7 days in 2-organ-chips provided by TissUse. The supernatant was sampled for further analysis of liver and islet functionality. At the end of the experiment, spheroids and islets were fixated for histological analysis. As other scientist were responsible for some of the analyses, such as those regarding the pancreatic islets, not all experiments involved in this project will be part of this thesis.

For this thesis, the expression of albumin from the liver spheroids was characterized by immunofluorescent staining and by measuring the levels of albumin secreted into the supernatant. The expression of the major metabolizing enzyme CYP3A4, the cytoskeletal protein vimentin present in stellate cells, and the protein α-SMA present in differentiated stellate cells were also characterized through immunofluorescent staining. The viability of the liver spheroids was determined by measuring the levels of lactacte dehydrogenase in the supernatant, an enzyme expressed intracellularly in the spheroids. Spheroids were also stained with hematoxylin and eosin to assess the possible formation of necrotic cores, as well as with periodic acid/Schiff staining to qualitatively evaluate the accumulation or possible depletion of glycogen storages.

1.3 Limitations

The size of the liver spheroids and the cellular fractions used to manufacture them have been determined in beforehand and will not be evaluated. The chips themselves will also not be evaluated. Since this thesis is part of a larger project, the section regarding the microfluidic devices has been restricted to focus on the functionality and characteristics of the liver spheroids. Suitable protocols for the culturing of spheroids and stellate cells, as well as for some of the analyses, will be created and optimized. All work on the 2-organ-chips will be performed in collaboration with other scientist at AstraZeneca. Analysis of pancreatic islets, as well as some analyses regarding the liver spheroids, such as gene expression, will be administered by another department at AstraZeneca and will not be part of this thesis. Furthermore, this thesis is restricted to only performing a semi-targeted analysis of the metabolites formed from the set of compounds from Iegre et al. [16], and will only include the Phase I metabolizing enzymes CYP1A2, CYP2C9, CYP2D6 and CYP3A4 for the separate metabolic activity analysis.

2. Theory

This chapter will introduce the theoretical framework for this thesis and provide an overview of some of the previous work within this area of research.

2.1 General anatomy and functions of the liver

The liver is one of the most complex and versatile organs in the body, with an extraordinary spectrum of functions. It is the second largest organ in the body, located beneath the diaphragm and weighs between 1200 to 1500 grams [2][17]. One of the main vital functions of the liver is to secrete bile and bile salts. Bile is a complex alkaline fluid that aids in the digestion and absorption of lipids and lipid-soluble vitamins and helps eliminate waste products (e.g. cholesterol).

Due to its location in the body, the liver is directly connected to the digestive system, supporting its crucial role in the processing of absorbed nutrients and xenobiotics. It is responsible for the synthesis of serum proteins (e.g. globulins, albumin, prothrombin, fibrinogen), intermediary metabolism of carbohydrates, lipids, proteins and amino acids, and detoxification of xenobiotic compounds. When blood glucose levels are high, the liver can convert glucose into glycogen and triglycerides for storage. Similarly, when blood glucose levels are low, the liver can break down the stored glycogen to glucose, which is released into the blood stream. Ammonia, a toxic side product from protein metabolism, is converted in the liver to urea, which is extrected in urine. Other vital functions of the liver include processing of hormones, excretion of bilirubin, storage of vitamins and minerals, and activation of vitamin D [18]. The liver also has a unique ability to regenerate after injury, inflammation and surgical resection compared to other organs, and is able to restore its original mass, cellular structure and function [2].

The liver is traditionally divided into two parts called the right and left lobes, separated by the falciforn ligament (Figure 2.1). Two different blood vessels provide the liver with a dual blood supply. The hepatic artery delivers oxygenated blood from the heart and provides approximately 25% of the liver's total blood supply. The portal vein delivers partially deoxygenated and nutrient-rich blood from the small intestine, which stands for about 75% of the total blood supply to the liver [19]. Throughout the liver, branches of the portal vein, hepatic artery and the bile ducts form structures called portal triads, consisting of one portal vein, hepatic artery and bile duct branch each. The liver can be further divided into functional units called lobules. These have three to six portal triads arranged around the perimeter and a central vein in the middle (Figure 2.2). The direction of the blood flow within the lobules is from the periphery to the center [2].

On histological sections, the liver appears as a homogenous and richly vascularized tissue [17]. However, on a microscopic level, it can be seen that the liver consists of a number of different cell types, which can be divided into parenchymal cells, or hepatocytes, and

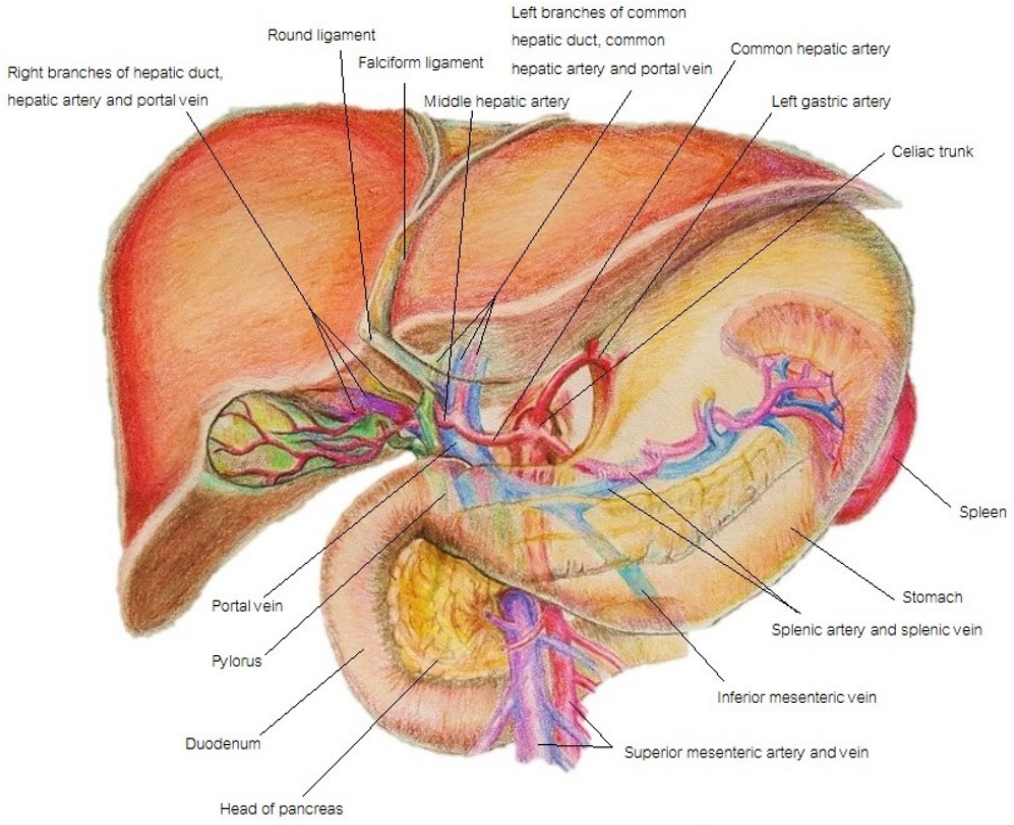

Figure 2.1: Antero-visceral view of the liver.

non-parenchymal cells. The latter include Kupffer cells (resident macrophages), sinusoidal endothelial cells, periportal fibroblasts, hepatic dendritic cells and stellate cells [2].

2.1.1 Hepatocytes

Hepatocytes are large polygonal cells making up approximately 60% of the total cell population and 80% of the total volume of the liver [17]. They are often seen as the functional units of the liver performing many of the functions associated with the liver. Normally, hepatocytes are structurally and functionally polarized, and have three distinct membrane domians known as the sinusoidal (basal), lateral, and canalicular (apical) domains. Basal surfaces form the sinusoidal blood vessels that branch between the portal vein and hepatic artery to the central vein. These are lined with endothelial cells, Kupffer cells and fat cells. Canalicular surfaces form the bile canalicular network that transports bile to the bile ducts. The lateral membranes form tight junctions with the bile canaliculi, occluding the apical domain and blood-bile barrier from the basolateral surface. Other connections, such as desmosomes, as well as intermediate and gap junctions, provide cohesive strength and functional communication between hepatocytes [2].

Within the liver lobules, hepatocytes are arranged in unicellular plates of about 20 cells with sinusoids separating each individual plate [17]. Every hepatocyte is in contact with the sinusoid walls through surrouding hepatocytes and through the perisinusoidal space (space of Disse), a space that separates the fenestrated endothelial cells present in the sinusoids from the hepatocytes, allowing for the hepatocytes to extend microvilli towards the blood vessels. This allows for bi-directional permeability and exchange of materials

from both hepatocytes and blood [2]. Depending on their physical location along the porto-central axis of the liver cell plate, the hepatocytes have been demonstrated to be specialized and perform different functions, despite being histologically indistinguishable [20].

2.1.2 Stellate cells

Non-parenchymal cells only comprise about 6% of the total liver volume, but almost 35% of the total cell number. Of these, 40% are fenestrated endothelial cells. Stellate cells constitute about 22% of the remainder of these cells. They are the main fat-storing cells in the liver and can be identified by the presence of intracellular vitamin A droplets (retinoids) and filamentous material. Stellate cells are normally situated around the sinusoids between endothelial cells and hepatocytes, or intercalated between hepatocytes [2].

Under normal physiological conditions, stellate cells are quiescent and long-lived, with spindle-shaped bodies. However, upon liver injury, stellate cells tend to become activated as a primary tissue repair response. The process of activation involves the cells disposing of their vitamin A storages while transdifferentiating to a more myofibroblast-like phenotype. The same type of phenotypical transformation and activation can be seen when stellate cells are grown on tissue culture plastics. Activated stellate cells are the major cause of liver fibrosis due to their excessive synthesis and release of extracellular matrix components [2][21]. Although activation of stellate cells often lead to perpetuation of their activated state through changes in cell behavior, the reversion of activated stellate cells to a more quiescent phenotype has been observed. *In vitro*, this can be achieved by transferring activated stellate cells to a basement membrane matrix. The mechanisms behind the reversion *in vivo* are still unclear [21].

Due to their ability to contract and relax in response to vasoactive mediators, stellate cells have an important role in sinusoidal blood flow regulation. This is particularly important during inflammation, when the sinusoids are narrowed to allow for longer interaction of microbes present in the blood with the innate immune cells (Kupffer cells), due to slower movement of the blood through the capillaries. Stellate cells are also able to produce a number of cytokines, chemokines, lipoproteins, and growth factors, as well as antigen-presenting and co-stimulatory molecules, giving them an important role not only in inflammation response and immunity, but also in hepatic growth [2][21].

2.1.3 Liver zonation

Based on oxygen and nutrient supply, the liver lobule can be divided into three zones. The area where the blood from hepatic arterioles and portal venules enter the lobule is zone 1, or the periportal area. Zone 3 is the area located around the central vein, known as the perivenous area, and zone 2 is located in between zones 1 and 3. Through this arrangement, blood rich in oxygen and nutrients reaches the cells in the periportal area first and then the cells located in the center of the lobule [2]. As mentioned above, hepatocytes are functionally different depending on their location along the portocentral axis, which is accounted for by this structural arrangement. Not all hepatic functions are strictly zonal, the synthesis of certain serum proteins such as transferrin appear to occur in all hepatocytes, with occasional preferences for certain zones. This functional zonation mainly affects glucose metabolism, ammonia detoxification, and xenobiotic metabolism. Some

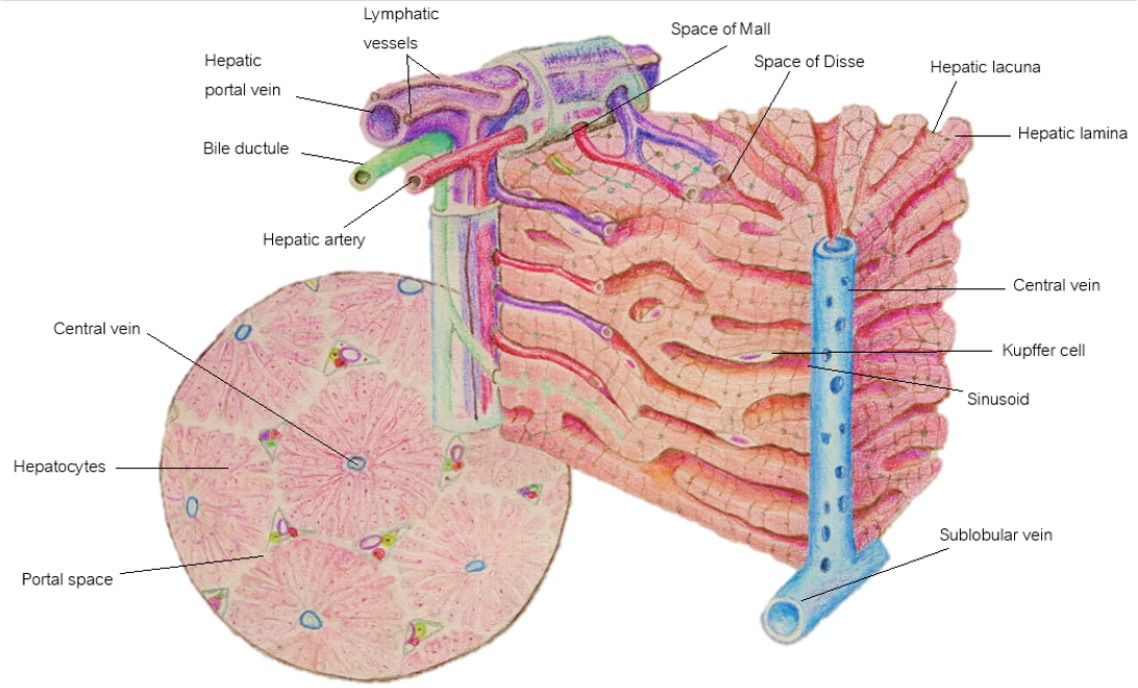

Figure 2.2: Illustration of a liver lobule.

other zonated processes include lipid metabolism, synthesis of bile acids, and metabolism of amino acids [2].

2.2 Drug metabolism

The body is exposed to a vast amount of chemicals every day, including drugs and pharmaceutical agents, household chemicals, and pollutants. Many of these chemicals can be directly harmful, while others need to be enzymatically processed to be effective. The liver is the main organ hosting the body's primary response against xenobiotics and other molecules, namely the drug metabolizing enzymes. The role of these enzymes is to modify the foreign compounds so that they can be excreted from the body more easily, typically by making them more hydrophilic [2][22].

The major chemical reactions involved in drug metabolism can be divided into hydrolysis reactions, reductions, oxidations, and conjugations. Traditionally, drug metabolism is divided into phases, where Phase I and Phase II are the major parts. Phase I reactions generally involve oxidations, reductions and hydrolysis to make the compounds more polar. These reactions are normally carried out by cytochrome P450 enzymes, flavin containing monooxygenases, and aldehyde and alcohol dehydrogenases, which are often classified as Phase I enzymes [22]. Phase II reactions mainly concern conjugations such as glucoronidations, glutathione conjugations, sulfations, methylations and acetylations, as well as amino acid conjugations. Examples of some Phase II enzymes include sulfotransferases, glucoronosyltransferases, acetyltransferases, and glutathione-S-transferase [23]. Lately, however, research has shown that in some cases, compounds are conjugated before becoming substrates for Phase I enzymes, or are excreted immediately after initial conjugation [2].

2.2.1 CYP450 enzymes

Cytochrome P450 enzymes (CYPs) function as monooxygenases and constitute the major enzyme family in the Phase I metabolism of xenobiotics and other lipophilic compounds. The oxidative metabolism executed by these enzymes can result in inactivation of drugs and facilitated elimination or metabolic activation of pro-drugs. The liver is the major site of CYP expression and the enzymes of greatest importance for drug metabolism belong to the familes 1-3, with CYP3A4 as the most abundant isozyme. These are responsible for 70-80% of all Phase I dependent metabolism of clinically relevant drugs [2]. Certain intrinsic and extrinsic factors can influence the expression and function of these enzymes, including genetic polymorphism, epigenetic influences and additional host factors such as sex, age and disease states [24]. Evaluation of CYP activity for measuring Phase I metabolism capacity in hepatocytes may include CYPs 1A2, 2A6, 2C8, 2C9, 2C19, 2D6, 2E1 and 3A4. This thesis will consider CYPs 1A2, 2C9, 2D6 and 3A4.

CYP1A2 is involved in the metabolism of xenobiotics through hydroxylations and other oxidative transformations. It has a preference for planar, aromatic, polyaromatic and heterocyclic amides and amines. The enzyme is expressed at relatively high levels in the liver and plays an important role in the metabolism and bioactivation of clinically important drugs. These include analgesics and antipyretics, antipsychotics, anti-inflammatory drugs, and cardiovascular drugs, such as omeprazol and carbamazepine. Endogenous substrates include arachidonic acid, prostaglandins, estrogens, melatonin and retinoic acid [24]. CYP1A2 has also been found to be involved in the bioactivation of certain procarcinogens present in charbroiled food and industrial combustion products, resulting carcinogenic intermediates able to cause DNA damage. It is therefore considered an important enzyme to test and evaluate [2][24]. CYP1A2 is sensitive to interactions from several small molecule inhibitors that fit the active site, capable of both reversible and irreversible inhibition, which can affect any drug treatment with CYP1A2 substrates [24].

CYP2C9 is the highest expressed member of the CYP2C family, which represents a significant fraction of the total P450s [24][25]. It accepts weakly acidic molecules with a hydrogen bond acceptor, which includes most non-steroidal anti-inflammatory drugs (NSAIDs). Endogenous substrates include arachidonic acid and certain steroids. Diclofenac and tolbutamide are the most common substrates used for CYP2C9 phenotyping and activity assays [24]. Genetic variation in the *CYP2C9* gene is a major cause of adverse drug reactions, since many of its substrates have a narrow therapeutic index [26].

CYP2D6 is expressed at relatively low levels in the liver, but is involved in the metabolism of a substantial amount of drugs from nearly all therapeutic classes, including antiarrhythmics, antidepressants, antipsychotics, β-blockers, and anti-cancer drugs. CYP2D6 is therefore considered to have a deep impact on human health in general [24][27]. Due to its extensive genetic polymorphism, the enzyme shows a very high degree of interindividual variability in its expression and function. The different resulting phenotypes can be divided into four groups based on metabolic activity, classified as either poor, intermediate, extensive, or ultra-rapid metabolizers. The consequences of the different phenotypes range from increased risk of adverse drug reactions for the poor metabolizers, to a lack of response for the ultra-rapid metabolizers [27].

CYP3A4 is the most abundantly expressed enzyme in the CYP3A subfamily, which plays a major role in the metabolism of almost 30% of clinically used drugs from all therapeutic

classes [24]. Its substrates consist of many large and lipophilic molecules of very diverse structures, including immunosuppressants, antibiotics, and anti-cancer drugs, as well as a range of smaller molecules. CYP3A4 is also involved in the hydroxylation of several steroids in the body, such as testosterone, progesterone, androstenedione, cortisol and bile acids [24].

2.3 Analysis of drug metabolism

Drug discovery and development typically involves screening and evaluating potential drug candidates to convert them to successful drugs. In order to spend minimal resources on poor candidates, early evaluation of these chemicals is crucial. Drug metabolism is therefore of great importance in medicinal chemistry and clinical pharmacology, due to the major impact of biotransformations and the resulting metabolites on the success or failure of drug candidates [28][29]. Some common aspects investigated include metabolic stability, CYP-reaction phenotyping, CYP inhibition and induction assays, detection of reactive metabolites, metabolite identification (MetID), determination of *in vitro* permeability, and estimation of plasma-protein binding [29]. This thesis will focus on metabolite identification.

2.3.1 MetID

Metabolite identification studies are relevant throughout the entire drug development process. At the discovery stage, MetID data can be used to identify sites on the compound that need to be modified or blocked, and eliminate those compounds that produce reactive or toxic metabolites. At a pre-clinical stage, MetID studies are used to help select animal species for toxicological and safety assessments. They also assist in the understanding of the mechanisms of action of the drug. Later in clinical trials, MetID is used for complete characterization of *in vivo* human metabolites [29][30]. During the early stages of drug development, however, one of the most important aspects of MetID studies is to identify the metabolites generated in different *in vitro* models, in order to predict what is likely to happen in the *in vivo* clinical trials [29].

The metabolism of a drug can be very complex; multiple enzymatic pathways involved can each produce different metabolites. Due to their chemical and physical diversity, MetID studies is an intrinsically difficult task. As a compound proceeds from discovery to pre-clinical (*in vitro*) to clinical (human *in vivo*) investigations, metabolite identification becomes even more challenging due to the complexity of the matrices (e.g. hepatocytes vs. blood plasma). Consequently, great efforts have been deployed over the past decade towards making metabolite identification better, faster and cheaper [30][31]. Mass spectrometry (MS) has thereby emerged as an optimal technique for the identification of the structurally diverse metabolites, greatly improving MetID studies through its high resolution and accurate mass determination capabilities [31][32].

2.3.2 LC-MS in drug metabolism analysis

Throughout the entire drug discovery and development process, mass spectrometry has become an essential tool for detecting and characterizing metabolites. Generally, MS is coupled to a separation system such as high-performance or ultra-high-performance liquid chromatography (HPLC or UPLC), generating a highly robust, rapid and sensitive

method for separating, detecting and structurally determining single molecules in complex mixtures [28][32]. The most time-consuming step in mass spectrometry, however, is interpreting the data generated to establish plausible molecular structures, which both requires an extensive library of experimental data, as well as previous experience, for efficiency [32][33].

Liquid chromatography allows for the separation of compounds with a wide range of polarity, and thereby facilitates metabolite identification when coupled to MS by reducing the sample complexity prior to detection [34][35]. Of the various types of chromatography available, reversed-phase liquid chromatography (RPLC) is the most commonly used method for metabolite profiling. For this method, a relatively non-polar stationary phase is used, such as C18-derived silica, along with a more polar mobile phase [28][36]. When separating mixtures of compounds with diverse properties, a gradient elution is most often applied, where the organic composition of the solvent is gradually increased. HPLC uses high pressure to force the solvent through a column containing a stationary phase made of very fine particles, which increases the efficiency and resolution of the separations [36].

The coupling of LC to MS tools utilizing atmospheric pressure ionization and electrospray ionization (ESI) has been a major step forward in MetID strategies, and are now the methods of choice for most studies detecting metabolites in complex biological samples [29][35]. Charged particles exhibit very precise dynamics when subjected to electrical and magnetic fields in a vacuum. This principle is taken advantage of in mass spectrometry, where particles are separated according to their mass-to-charge ratio (m/z), from which the mass can then be deduced [36][37]. Certain types of mass spectrometers, such as time-of-flight (TOF) MS or Fourier transform ion cyclotron resonance (FT-ICR) instruments are accurate enough to be able to derive empirical atomic formulas for the compounds detected. To further analyze ions of interest, tandem mass spectrometry (MS/MS) can be performed, from which further structural information can be obtained from the resulting fragmentation patterns of the metabolite(s) [28][32].

Depending on whether a study to identify metabolites can be classified as targeted, semi-targeted, or untargeted, different analysis strategies might be applied. Unlike untargeted analysis, during targeted and semi-targeted analyses, the chemical identities of all or most metabolites to be assayed are known in beforehand, and common structures are already collected in online databases [33][38]. The data from any LC-MS study is often generated as concentration versus time, and the masses deducted from the m/z ratios detected are compared to the available data in the metabolite libraries. Nevertheless, verifying structures and identifying metabolites is yet a time-consuming process that often requires previous experience, and is the typically the largest bottleneck in metabolite identification [32].

2.4 *In vitro* liver models

Tissue engineering in general aims to provide novel therapies for certain organ diseases and create models for understanding fundamental aspects of human biology and diseases. One important aspect is the development of *in vitro* liver culture platforms. Such models can be used to study fundamental hepatocyte biology, understand and develop solutions for liver pathophysiology, and evaluate the metabolism and toxicity of pharmaceutical compounds [2]. The latter is of high importance to the pharmaceutical industry, where

drug-induced liver injury (DILI) at later stages is a major problem.

Current techniques used to evalute the aforementioned parameters prior to pre-clinical trials, such as animal models, do not detect all potentially harmful compounds. These discrepancies can often be explained by differences in metabolism or host-specific responses, or that the animal models cannot reflect human cell interactions. Also, *in vivo* studies performed in animal models typically use very high doses of compounds, and normally do not test mixtures of compounds, whereas humans are often subjected to complex cocktails of substances [39][40][41]. The inability of the models to predict drug toxicity at an early stage leads to huge financial losses, as well as retractions of certain drugs from the market. By developing and improving the abilities of these models to more accurately simulate the human *in vivo* metabolism and liver biology, the drug development process could become more cost-effective as well as reducing the need for animal testing [39][42].

An optimal cell model should have an *in vivo*-like phenotype and be able to mimic a multicellular tissue in culture. It should also be suitable for high-throughput screening and generate quantitative, reliable data for *in vivo* predictions of human pharmacodynamics and pharmacokinetics as well as toxicology [43]. No such model currently exists, rather, different cell models have different benefits and limitations depending on the type of analysis and what data is required. Current models mostly consist of immortalized cell lines and primary hepatic cells, isolated microsomes, and liver slices [41]. Lately, several strategies for three-dimensional cell cultures have been developed as well, including growing cells between ECM-like matrices, spheroid formation, bioreactors, and multi-organ chips [42].

2.4.1 Cell lines and primary cells

For all liver models that currently exists, multiple cell sources are available. The most common cell types are polarized hepatoma cell lines and primary cells. Primary human hepatocytes (PHH) are generally considered as the most relevant system for *in vitro* liver enzyme function, drug metabolism and toxicity assays [2][43]. They are functionally more representative of the liver than cell lines, for instance since they express all endogenous hepatic transporters, and can be cryopreserved to overcome inter-donor variablility. However, PHH are notoriously difficult to maintain in culture due to their rapid decline in viability, dedifferentiation, and the decrease in liver-specific functions in conventional suspension and 2D-cultures [2][39][43].

Hepatoma-derived cell lines are valuable alternatives for PHHs in many functional and metabolic studies. One of the most commonly used liver cell lines is HepaRG, established from a liver tumor of a female suffering from hepatitis C and hepatocarcinoma [44]. Hepatoma-derived cells often display irregular levels of certain hepatic functions, or lack them completely. However, they are also to a high degree reproducible and affordable models of hepatic tissues [43]. The HepaRG cell line is able to differentiate into two different cell types; hepatocytes or biliary epithelial cells. Under optimal conditions, HepaRG cells are able to express various types of metabolizing enzymes at levels comparable to PHH. They also express several drug transporters, nuclear receptors and membrane transporters, and are able to maintain a stable phenotype in culture for weeks [41][43][45].

The simplest approaches to create an *in vitro* liver model using either PHH or a cell line are suspension and monolayer cultures. Suspension cultures are mainly used with PHH, which are useful for estimating the rate of internal clearance of compounds, and normally

has a high throughput. However, the lack of cell-cell and cell-matrix contact quickly results in loss of cell polarity, integrity and differentiation after just a few hours [41][42]. Monolayer cultures are instead the most frequent method for short-term drug screening and enzyme induction assays. Cells are normally grow on ECM- or polymer-coated dishes, where collagen type I is the most common choice. This normally influences the phenotype of the cells more positively compared to suspension cultures, and can induce cell polarity and more stable mRNA expression. However, dedifferentiation usually occurs within 24-72 hours, leading to drastic decreases in cell functionality [2][42].

2.4.2 Three-dimensional liver models

The microenvironment of the hepatocytes *in vivo* can be complex to imitate. However, the maintenance of normal cell function and phenotype strongly depends on the cell-cell and cell-matrix interactions in the 3-dimensional tissue. Therefore, various attempts to create more complex culture systems better mimicking the native microenvironment of the hepatocytes have been developed. These include sandwich cultures on ECM or ECM-like polymers, scaffold-based systems and bioreactors [41]. All these models aim at recreating the correct cell phenotype, which should ideally include functional cell polarization, normal metabolic and transporter activity, as well as correct cell morphology. Nevertheless, these systems suffer from drawbacks such as lack of scalability, difficulties in manufacturing and handling, and lack of reproducibility [8][43].

To circumvent some of these problems, a 3D liver spheroid model has been developed. These microtissues closely resemble the ultra-structure of the *in vivo* liver lobule, and have been shown to be able to be maintained for longer periods of time with stable viability and functional cell polarity [8][42]. Spheroids are normally formed either by culturing the cells on a polymer-coated surface that induces spontaneous spheroid formation, or increasing cell-cell interactions by physical means and thereby inducing cell aggregation. The latter method includes techniques such as the hanging drop method, rotational agitation, or gel entrapment [42][43].

Another important aspect to consider is the fact that the liver functions by complex interactions and signaling from many different types of cells. Hepatocytes by themselves do not fully represent the functionality seen *in vivo*. Therefore, co-cultures with non-parenchymal cells is one of the most common methods to improve the *in vitro* microenvironment [41][43]. Studies have shown that three-dimensional co-cultures of hepatocytes and stellate cells are able to preserve certain aspects of hepatocyte function such as albumin and CYP450 expression, as well as improving the spheroid architecture, creating bile canaliculi, desmosomes, and tight junctions [46][47].

2.5 Microfluidic organs-on-chips

Understanding human pathophysiology and the tissue-specific, differentiated functions of cells, as well as accurately predicting *in vivo* tissue functions and drug metabolism, requires insight into how cells and tissues function in the context of whole living organs and organ systems. To better represent the tissue heterogeneity and 3D architecture of organs, increased efforts towards developing cell culture models including multiple cell types, 3D structures and extracellular-like matrices, as described above, have been made. Despite these considerable technological advances, however, current cell culture models

still fail to fully simulate the *in vivo* microenvironment. Difficulties to quantify transcellular transport, absorption and secretion often occurs due to issues sampling luminal contents and the variability in size and cellular positions of 3D models. Although being much more analogous to normal tissue architecture, many 3D models still lack certain tissue-tissue interfaces, such as the interfaces between vascular endothelium, connective tissue and parenchymal cells. Also, cells normally experience mechanical cues such as fluid shear stress, tension and compression, influencing organ development and function, an important aspect which is usually missing in current cell culture models.

The concept of organs-on-chips offers a possibility to overcome these limitations. Organs-on-chips are microfluidic cell culture devices created using a modified form of photolithography etching commonly used to manufacture computer chips, hence the word "chip". Microfludic culture systems are typically constructed by pouring a liquid polymer, preferably with a high gas permeability when solid such as polydimethylsiloxane (PDMS), onto an etched silicon base. The PDMS is then allowed to polymerize into an optically clear, rubber-like material, replicating the patterns on the silicon chip. [7][10][12][48]. This mode of fabrication allows for intricate control of surface feature shapes and sizes, on the same scale that is sensed by cells in their natural environment. Cells cultured in the chips can then be arranged in the continuously perfused chambers to simulate tissue- and organ-level functions. The goal is to synthesize minimal functional organ units rather than building whole living organs.

2.5.1 Control over parameters

Microfluidic chips can provide control over many parameters not easily controlled in static cultures or bioreactors by the integration of microsensors [49][50][51]. These microsensors can report on the cultured cells or microenvironmental conditions, such as fluid pressure, cell migration and barrier integrity. Control over fluid flow is enormously useful in many aspects. Due to the small size of the chambers and channels, and the fact that viscous forces dominate over inertial ones at small length scales, the flow in the chips is most often laminar, allowing for the generation of physical and chemical gradients [7][10]. Fluid shear stresses can even be controlled independently of these gradients by altering the flow rate or channel dimensions,or the overall channel or chip design.

Cells can also be plated in distinct patterns between porous substrates acting as barriers, allowing for the study of barrier function and transcellular transport, absorption and secretion. This is useful for mimicking certain tissue-tissue interfaces such as the interactions between vascular endothelium and parenchymal tissues. Chips can further be constructed to allow for mechanical environmental cues such as cyclic strain to be produced as well [52]. Other conditions that could be monitored with the development of more sensors include glucose, lactate and oxygen levels, and pH.

2.5.2 Modeling organ-level functions and disease

Microfluidic organs-on-chips are exceptionally relevant for studying basic mechanisms and biological phenomena of organ physiology and disease that depend on tissue microarchitecture and perfusion. However, since organs are normally composed of several different tissues, which are themselves constructed of various cell types, the combination of two or more cell or tissue types is often necessary to maintain crucial cell-cell interactions. Several devices have been developed over the past decades for the liver

[5][53][54][55][56][57][58][59][60][61][62][63][64][65][66][67][68], as well as other organs, such as the lung, the kidney, and even the brain [52][69][70]. Some of these are not as adequate organ models than others, since they only include one cell type in a 2-dimensional layer, but rather revealed important information regarding the effects of fluid flow and shear stress on cellular form and function. The studies performed on these devices have shown that gradients of oxygen and growth factors caused by fluid flow are the major sources of zonation, that the heterotypic cell-cell interactions stabilize hepatocyte function and metabolism, improving the predictivity of drug metabolism and toxicity assays, and that flow-based chips are superior for dynamic monitoring of metabolite production, to highlight some examples.

Due to the phylogenetic distance between animals used in laboratory testing and humans, it is very difficult to assess whether there are meaningful differences in drug uptake and metabolism between the animal model and humans. This is why the development of new solutions such as organs-on-chips has been of such great importance for studying the administration, distribution, metabolism, elimination, and toxicity (ADMET), as well as pharmacokinetics and pharmacodynamics. Nevertheless, these studies are still limited by the lack of organ cross-talk, failing to emulate the systemic organ complexity *in vivo*. This gave rise to the formation of multi-organ-chips, introducing the intriguing possibility to eventually create a "human-on-a-chip" [12][13][14][15][68]. These systems have reported on long-term co-cultures displaying tissue crosstalk, oral and systemic administration of drugs as well as systemic sensitivity to substances different from single-tissue cultures. The four-organ-chip developed by Maschmeyer et al. [14] with both a flow circuit interconnecting all four tissue compartments containing a skin, liver, gut, and kidney model, as well as a second circuit mimicking excretion through the kidney epithelial cells, is a first approach to establish a microfluidic system for *in vitro* long-term ADME profiling and systemic toxicity testing.

3. Materials and methods

The two parts of this thesis both consist of several individual experiments. These will be described in more detail in this chapter.

3.1 Materials

Cryopreserved differentiated HepaRG cells, ADD670 thawing and seeding additive and ADD620 maintenance additive were purchased from Biopredic International (Saint Grégoire, France). Cryopreserved primary human hepatocytes (PHH) and primary human hepatic stellate cells (SteC), as well as InVitroGRO CP medium and Torpedo antibiotics mix were purchased from Bioreclamation IVT (Westbury NY, USA). Ultra-low attachment (ULA), round bottom 96- and 384-well plates and ULA flat bottom 24-well plates, as well as tissue culture treated T75 cell culture flasks and non-treated T25 cell culture flasks were purchased from Corning (Flintshire, UK). Human hepatic stellate cell growth medium (HSGM) was obtained from ZenBio (Research Triangle Park NC, USA). Conical and flat bottom 96-well polystyrene Nunc plates, William's Medium E (WME), fetal bovine serum (FBS), phosphate buffered saline (PBS) pH 7.4 (-$CaCl_2$/-$MgCl_2$), GlutaMAX, HEPES (2-[4-(2-hydroxyethyl)piperazin-1-yl]ethanesulfonic acid) buffer solution, TrypLE Select, human recombinant insulin zinc solution, insulin-transferrin-selenium (ITS), gentamicin, penicillin-streptomycin (10 000 U/mL), Hoechst trihydrochloride, trihydrate 10 mg/mL solution, mouse monoclonal anti-human serum albumin antibody and Pierce LDH cytotoxicity assay kit were purchased from ThermoFisher Scientific (Uppsala, Sweden). Dexamethasone, L-glutamine, Trypan Blue solution (0.4%), hydrocortisone hemisuccinate (HC/HS), poly-L-lysine (PLL) solution, Triton-X, bovine serum albumin (BSA), Fluoromount aqueous mounting medium and 4'-hydroxydiclofenac were purchased from Sigma Aldrich (Stockholm, Sweden). Acetonitrile (ACN) and formic acid (FA) (Optima LC-MS-grade) were obtained from Fisher Scientific (Gothenburg, Sweden). Stellate cell medium and supplements were purchased from ScienCell (Carlsbad CA, USA). Human albumin ELISA kit, rabbit polyclonal anti-human cytochrome P450 3A4 anitbody, rabbit polyclonal anti-human alpha smooth muscle actin antibody and mouse monoclonal anti-human vimentin antibody were purchased from Abcam (Cambridge, UK). Paraformaldehyde (4% in PBS) was obtained from VWR (Gothenburg, Sweden). Glass coverslips were purchased from HistoCenter (Gothenburg, Sweden). Phenacetin, midazolam, bufuralol, diclofenac, paracetamol, 1'-hydroxymidazolam, 1'-hydroxybufuralol, as well as the compounds used for all MetID experiments were obtained from Compound Management at Astra Zeneca, Mölndal. Microfluidic 2-organ-chips and corresponding external pumps were purchased from TissUse GmbH (Berlin, Germany).

3.2 MetID experiments

This section will further explain the experimental procedures regarding the MetID experiments, including spheroid culturing, sampling and analysis.

3.2.1 PHH spheroid cultures

Cryopreserved PHH were used for the formation of spheroid cultures for these experiments. Cells were thawed in a 37 °C waterbath and immediately transferred to 5 mL PHH thawing medium (Table 3.1). The cells were then centrifuged at 80 x *g* for 5 minutes, after which the supernatant was removed and the cell pellet was dissolved in a small volume of PHH seeding medium. Cells were counted in a Bürker chamber and their viability was assessed using the Trypan Blue exclusion method. The cells were subsequently diluted in PHH seeding medium to a concentration of 20 000 cells/mL. The diluted cell suspension was thereafter seeded into ULA round bottom 96-well plates; 100 μL was transferred to each well equal to 2000 cells per well. Plates were centrifuged at 100 x *g* for 5 minutes and incubated at 37 °C, 5% CO_2. On day 4 after seeding, when the spheroids were sufficiently compact, 50% of the medium was exchanged for fresh PHH culturing medium. Spheroids were thereafter maintained in the serum-free culturing medium until further use, with a medium change every 48-72 hours.

Table 3.1: Different media used and their compositions.

Name	Base	Supplements	Supplement conc.
PHH thawing medium	InVitroGRO CP	Torpedo antibiotics	2.2%
PHH seeding medium	WME	FBS	10%
		L-glutamine	2 mM
		ITS	1%
		Pen-Strep	1%
		Dexamethasone	100 nM
PHH culturing medium	WME	L-glutamine	2 mM
		ITS	1%
		Pen-Strep	1%
		Dexamethasone	100 nM
MetID incubation medium	WME	HEPES	25 mM
		GlutaMAX	1%
		Pen-Strep	0.1%
Stellate cell medium	SteC basal medium	FBS	2%
		Pen-Strep	1%
		SteC growth suppl.	1%
HepaRG thawing medium	WME	GlutaMAX	1%
		ADD670	1 vial/ 100 ml
Chip medium	WME	FBS	10%
		L-glutamine	2 mM
		Insulin	5 μg/ml
		HC/HS	50 μM
		Gentamicin	1%

3.2.2 Compound incubation and sampling

On day 7 after seeding, spheroids were pooled 10 by 10 into the wells of an ULA round bottom 96-well plate, one well for each compound and sampling time point. The substrate compound stocks were available dissolved in DMSO at a concentration of 10 mM. These were diluted in MetID incubation medium (Table 3.1) in separate vials to a concentration of 4 μM. All of the residual medium was removed from the pooled spheroids, upon which they were washed once with PBS. Subsequently, all of the remaining PBS was removed and 100 μL of the compound solutions were added to their corresponding wells. MetID incubation medium without any compounds was also added to some wells to serve as a blank. The supernatants and the spheroids were sampled at 6 different time points; 0, 4, 8, 24, 48 and 72 hours after addition of the compounds. At each timepoint, 50 μL of the supernatants were sampled and quenched in 100 μL STOP solution (100% ACN with 0.8% FA) for each sample in a separate plate on dry ice. The remaining supernatants were removed, after which spheroids were washed in PBS, sampled in 50 μL fresh MetID incubation medium without any added compounds, and quenched in 100 μL STOP solution in another plate on dry ice. The plate with the remaining spheroids was incubated at 37 °C, 5% CO_2 along with the remaining compound dilutions. These remaining dilutions were also sampled as described above alongside the cell incubations, either at time points 0 and 72 hours, or at all time points, to verify whether the original compound contained any impurities and if it was unstable in the cell medium at 37 °C. Sample plates were covered with rubber lids and stored at -80 °C in between sampling time points and analysis.

3.2.3 Sample analysis

The cell sample plate was freeze/thawed for 2-3 cycles with vigorous shaking in between each cycle to disrupt the cells and release any internal compounds. Afterwards, both plates were thawed and centrifuged at 4000 rpm and 4 °C for 20 minutes to allow for all cell debris to sediment. The supernatants in both plates were then diluted 1:1 in dH_2O in two separate conical bottom 96-well Nunc plates. The plates were covered with rubber lids and analyzed by LC-MS.

3.2.4 CYP activity

Alongside one of the MetID experiments, a CYP activity assay was performed on cell suspension and spheroids from the same batch of cells. On the same day as the cells were thawed and seeded (day 0), some of the cell suspension was seeded into a flat bottomed 96-well plate. Each well contained 50 μL cell suspension at a concentration of 200 000 cells per mL, equal to 10 000 cells per well, in 5 replicates. A CYP cocktail was prepared according to Table 3.2 in WME. Each well was incubated with 50 μL of the cocktail at 37 °C, 5% CO_2. After incubating the samples for 4 hours, the activity was quenched by transferring 50 μL of the supernatant of each sample into 100 μL STOP solution containing 4 nM of internal standard #39 (5,5-dimethyl-1,3-diphenyl-2-iminobarbituric acid) on a separate 96 well plate on dry ice. The plate was covered with a rubber lid and stored at -20 °C until analysis.

On day 7 (start of the MetID experiment) and day 10 (end of the MetID experiment), spheroids were pooled 5 by 5, in 5 and 2 replicates respectively, in separate plates. The spheroids picked on day 7 had been maintained as described in section 3.2.1, and the spheroids picked on day 10 had also been maintained in MetID incubation medium without any added compounds (similar to the blank MetID samples) between days 7-10. All

Table 3.2: CYP cocktail composition and targets.

Substance	CYP ligand	Cocktail conc. (μM)	Final conc. (μM)
Phenacetin	CYP1A2	52	26
Midazolam	CYP3A4	6	3
Bufuralol	CYP2D6	40	20
Diclofenac	CYP2C9	18	9

excess medium was removed from the spheroids and 50 μL WME without any additional substances was added to each well. CYP cocktail was subseqently added to each well, and the samples were treated as described above. Before analysis, all samples were diluted 1:2 in dH_2O in a conical bottom 96 well Nunc plate. A standard curve of the primary metabolites paracetamol, 1'-OH-midazolam, 1'-OH-bufuralol, and 4'-OH-diclofenac was added to the plate as well, and the samples were analyzed by LC-MS/MS (Triple Quadrupole).

3.3 Chip experiments

This section will further explain the experimental procedures concerning the 2-organ chip experiments, including stellate cell culturing, spheroid formation, chip culturing and management, and sample analysis.

3.3.1 Stellate cell culturing

Stellate cells were cultured in two sessions to establish a proper culturing protocol. For the first session, PLL coated and non-coated T25 culture flasks were used, as well as HSGM and PHH thawing medium (Table 3.1). To manufacture the PLL-coated cell culture flasks, poly-L-lysine was dissolved in sterile tissue culture grade water to a concentration of 0.1 mg/ml. Non-coated T25 cell culture flasks were then coated with 1 mL PLL per 25 cm^2. The coating was allowed to set for 5 minutes, after which the flasks were washed with sterile water and allowed to dry for 2 hours.

Cryopreserved human hepatic stellate cells were thawed in a 37 °C water bath and immediately transferred to 5 mL PHH thawing medium. The cells were centrifuged at 80 x g for 5 minutes, the resulting supernatant was removed and the cell pellet was dissolved in a small volume of PHH thawing medium. Cells were counted in a Bürker chamber and their viability was assessed using the Trypan Blue exclusion method. Half the cell suspension was then further diluted in PHH thawing medium, while the other half was diluted in HSGM. The cells diluted in PHH thawing medium were seeded at a density of 4000 cells/cm^2 in both non-coated and PLL-coated T25 cell culture flasks. The cells diluted in HSGM were seeded in the same type of flasks at the same density. The flasks were incubated at 37 °C, 5% CO_2 for 12 hours. The next day, the medium in all flasks were exchanged for fresh PHH thawing medium or HSGM to remove any residual DMSO and unattached cells. The cells were monitored every 24-48 hours under a bright-field microscope to evaluate their viability and proliferation, and the medium was changed every 48-72 hours.

Since only the cells cultured in HSGM were able to survive and proliferate, all further experiments were conducted on these cells. After reaching a confluency of approximately 90%, the cells were trypsinized and subcultured in new flasks. When subculturing the cells, all culture medium was removed from the flasks and the cells were washed gently

in PBS to remove any traces of serum, calcium, and magnesium that could inhibit the action of the dissociation reagent. After discarding the PBS, 0.5 mL TrypLE was added per 10 cm^2 and the flasks were incubated at 37 °C for 2 minutes. Afterwards, the cells were observed under a microscope. When more than 90% of the cells had detached, twice the volume used for the dissociation agent of HSGM was added to the flasks, the liquid was transferred to a Falcon tube, and the cells were centrifuged at 80 x g for 5 minutes. The resulting supernatant was removed and the cell pellet was dissolved in a small volume of HSGM. The cells were counted in a Bürker chamber and their viability was assessed using the Trypan Blue exclusion method. Afterwards, the cells were further diluted in HSGM, the cells were seeded into new flasks, either PLL-coated or non-coated T25 cell culture flasks, at a density of 4000 cells/cm^2, and the flasks were incubated at 37 °C, 5% CO_2. The next day, the medium was exchanged to fresh HSGM, after which the medium was changed every 48-72 hours.

For the second culture occasion, tissue culture-treated T75 culture flasks were used, as well as stellate cell medium (Table 3.1). Cryopreserved human hepatic stellate cells were thawed as described above, except that stellate cell medium was used to dissolve the pellet after centrifugation instead of PHH thawing medium. After counting the cells, the cell suspension was further diluted in stellate cell medium, and the cells were seeded into tissue culture-treated T75 culture flasks at a density of approximately 13 000 cells/cm^2 in 10 mL medium. The cells were thereafter incubated at 37 °C, 5% CO_2 and maintained by changing the medium the day after seeding and consequently every 48-72 hours. Cells were also monitored daily under a microscope to examine their proliferation. After reaching a confluency of roughly 80%, the cells were subcultured as described above, except that stellate cell medium was used instead of HSGM. After centrifugation, the cells were counted and split 1:4 into new tissue culture-treated T75 culture flasks.

3.3.1.1 Stellate cell immunocytochemistry

During the first culturing occasion, some cells cultured in HSGM were stained via ICC for two protein markers. When passaging the cells, some of the cell suspensions from both types of flasks were seeded into separate wells of a black-walled flat bottomed 96-well plate at a concentration of roughly 20 000 cells per well. The cells were incubated overnight at 37 °C, 5% CO_2 to allow for them to attach to the plate. Afterwards, the cells were washed with PBS and fixated by incubating them in 4% paraformaldehyde in PBS at room temperature for 20 minutes. The cells were then washed twice with PBS and permeabilized by incubating the samples with 0.5% Triton-X in PBS for approximately 30 minutes.

After permeabilizing the cell membranes, the cells were incubated with a blocking buffer, consisting of 10% BSA dissolved in PBS for 45 minutes. The blocking buffer was then removed, and without washing in between, the samples were incubated with primary antibodies for vimentin and α-SMA diluted in blocking buffer according to Table 3.8 for 3 hours at room temperature. The samples were subsequently washed 3 times in PBS for 5 minutes each and incubated with the respective secondary antibodies (Table 3.8) diluted in PBS for 45 minutes at room temperature in the dark. Since the secondary antibodies were conjugated to fluorescent markers, all subsequent steps were also performed in the dark. The cells were washed 3 times in PBS for 15 minutes each, after which cell nuclei were counterstained by incubating the samples with Hoechst diluted in PBS to a concentration of 0.625 μg/mL for 1 minute. The samples were washed once more in PBS for 5 minutes and the plate was stored wrapped in aluminum foil at 4 °C until visualization under a

confocal microscope.

3.3.2 HepaRG/SteC co-culture spheroids

In total, 5 chip experiments using HepaRG/stellate cell co-culture spheroids were performed. Four of these experiments used spheroids made only from freshly thawed cryopreserved cells, while one of them used both freshly thawed cryopreserved cells and cryopreserved cells that had been precultured.

For the first 4 experiments, cryopreserved differentiated HepaRG cells and cryopreserved primary human stellate cells were thawed in a 37 °C waterbath on the same day as they were seeded into aggregates. The HepaRG cells were then immediately transferred to 10 ml HepaRG thawing medium (Table 3.1) per vial thawed, while the stellate cells were immediately transferred to 5 mL PHH thawing medium. The HepaRG cells were centrifuged for 3 minutes at 500 x *g* and the stellate cells were centrifuged for 5 minutes at 80 x *g*. The resulting supernatants were removed and the cell pellets were resuspended in small volumes of chip medium (Table 3.1). The HepaRG cells and the stellate cells were counted separately in Bürker chambers and the viability of the cells were assessed using the Trypan Blue exclusion method.

A joint dilution in chip medium of the two cell types was then created. For the first 3 experiments, the suspension contained HepaRG cells at a concentration of 240 000 cells/mL and stellate cells at a concentration of 10 000 cells/mL. The cell suspension was seeded into ULA round bottom 96-well plates; 100 μL was transferred to each well equal to 25 000 cells per well. Plates were centrifuged at 100 x *g* for 5 minutes and incubated at 37 °C, 5% CO_2 without shaking. For the 4th experiment, a dilution with HepaRG cells at a concentration of 480 000 cells/mL and stellate cells at a concentration of 20 000 cells/mL was prepared. The cell suspension was seeded into ULA round bottom 384-well plates; 50 μL was transferred to each well equal to 25 000 cells per well. The plates were centrifuged at 100 g for 5 minutes and incubated at 37°C, 5% CO_2 without shaking for three days and were thereafter placed on an orbital or wave shaker for one day.

For the 5th experiment, two types of spheroids were prepared; one type consisting of cells that had been thawed on the same day as they were seeded, and one type consisting of cells that had been precultured prior to seeding them into aggregates. For the precultured cells, stellate cells had previously been thawed and cultured in tissue culture-treated T75 cell culture flasks as described in section 3.3.1. Four days prior to seeding the aggregates, HepaRG cells were thawed as described above, except that the cell pellet was resuspended in HepaRG thawing medium (Table 3.1). Approximately 15 million cells were then seeded in 12 mL medium into a T75 collagen I-coated cell culture flask, which was incubated at 37 °C, 5% CO_2. The next day the medium in the flask was exchanged for HepaRG maintenance medium, which is similar to HepaRG thawing medium except that it contains ADD620 supplement instead of ADD670.

On the day when the cells were seeded into spheroids, the precultured HepaRG cells as well as precultured stellate cells of passage 4 were trypsinized as described for subculturing stellate cells in section 3.3.1. After the cells had detached, chip medium was added to the flasks and the cells were collected in separate Falcon tubes. Cryopreserved differentiated HepaRG cells and human primary stellate cells were thawed as described above. All cells were thereafter counted in Bürker chambers and their viability was assessed using the

Trypan Blue method. Two separate dilutions were prepared, one with the precultured cells and one with the freshly thawed cells. In both cell suspensions, HepaRG cells were added to a concentration of 480 000 cells/ml and stellate cells were added to a concentration of 20 000 cells/mL. The two cell suspensions were seeded into separate ULA round bottom 384-well plates, equal to 25 000 cells per well. The plates were centrifuged at 100 x g for 5 minutes and incubated at 37 °C, 5% CO_2 without shaking for 2 days, and then on a wave shaker for an additional 2 days.

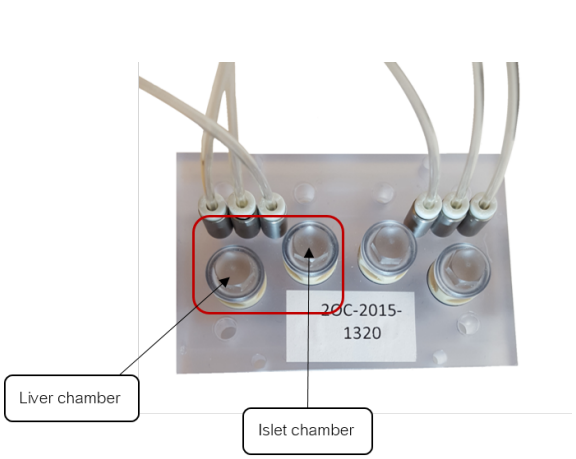

(a) Outline of a circuit on the 2-organ chip.

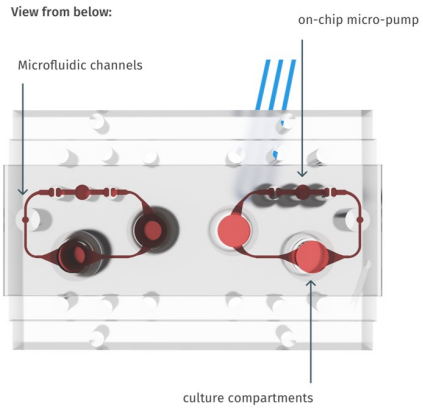

(b) Illustration of a 2-organ chip as seen from below.

Figure 3.1: Images of circuits on a 2-organ chip seen from above and below. **(a)** Outlined is one circuit with its respective organ chambers indicated, classified as one replicate in the chip experiments. One chip is able to contain two separate replicates. **(b)** Outlined are the microfluidic channels connecting the culture compartments in the circuits. Image courtesy of TissUse GmbH.

3.3.3 Multi-organ chip culturing

A general protocol for conducting experiments using the 2-organ chips was provided by TissUse GmbH. The protocol was altered slightly for each run to fit the purpose of the individual experiment. Once the liver spheroids, and for 3 of the experiments pancreatic islets, had been inserted into the chips, each experiment (labeled Chip 1-5) lasted for 7 days.

In general, 4 days after seeding the liver spheroids, the aggregates were pooled 40 by 40 in low insulin chip medium in ULA flat bottom 24 well plates and incubated overnight at 37 °C, 5% CO_2. The chambers of the chips were washed twice with PBS, after which they were each filled with 300 μL chip medium without insulin. The chips were attached to the pumps, and the medium was allowed to circulate through the circuits overnight. The next day, the liver aggregates were washed with insulin-free chip medium and incubated in the insulin-free medium for 2 hours at 37 °C, 5% CO_2. The chips were disconnected from the pumps, and the medium in the chambers was replaced with fresh insulin-free chip medium with any relevant additions. Forty liver spheroids, equivalent to 1 000 000 cells, and 10 pancreatic islets were added to each relevant chamber, and the chips were reattached to the pumps and incubated at 37 °C, 5% CO_2. Media samples were typically taken from the chips at 0, 4 and 24 hours from day 0 and day 6. The media in the chips were exchanged every 24-48 hours as specified for each experiment. On day 7, after finishing the experiment, the liver spheroids were taken out of the chambers, fixated in 4%

paraformaldehyde in PBS and sent off to HistoCenter for sectioning.

The purpose of the first chip experiment was to test the effect of different glucose concentrations on liver spheroids and pancreatic islets. For this experiment, chip media with 3 different glucose concentrations (1, 1.5 and 2 g/L) were prepared. The experiment was conducted according to the general protocol with some exceptions. After washing the chips, the chambers were filled with medium containing the relevant glucose concentration. Spheroids were picked and pooled 3 days after seeding the aggregates, and were washed in the medium they were to be incubated in without further incubation before seeding them into the chips. The different media in the chambers were exchanged every 48 hours.

Table 3.3: Chip 1 experimental setup.

Chip no.	Circuit	Treatment	Cell culture
1	A	2 g/L glucose	Liver and pancreas
1	B	2 g/L glucose	Liver and pancreas
2	A	2 g/L glucose	Liver and pancreas
2	B	2 g/L glucose	Liver and pancreas
3	A	1.5 g/L glucose	Liver and pancreas
3	B	1.5 g/L glucose	Liver and pancreas
4	A	1.5 g/L glucose	Liver and pancreas
4	B	1.5 g/L glucose	Liver and pancreas
5	A	1 g/L glucose	Liver and pancreas
5	B	1 g/L glucose	Liver and pancreas
6	A	1 g/L glucose	Liver and pancreas
6	B	1 g/L glucose	Liver and pancreas

The purpose of second chip experiment was to test the effects of S961, a peptide known to induce insulin resistance in rats [71], as well as Exenatide-4 (Ex-4, a GLP-1 receptor agonist) on liver spheroids and pancreatic islets. All of the following experiments used chip medium with a 2 g/L glucose concentration. The experiment was conducted according to the general protocol with some exceptions. Spheroids were pooled in regular chip medium and incubated overnight. 50% of the media were exchanged every day, except for on day 6, when 100% of the media were exchanged. Since S961 levels were estimated to deplete significantly over 24 hours, each time 50% of the media were exchanged, the fresh media contained twice the final desired concentration of S961. Ex-4 was only added to the chips on days 0 and 6, when 100% of the media were renewed. Between days 3-6, 5-ethynyl-2'-deoxyuridine (EdU) was added at a concentration of 10 μM to the designated circuits to stain the pancreatic islets.

Table 3.4: Chip 2 experimental setup.

Chip no.	Circuit	Treatment	Cell culture
1	A	200 nM S961	Liver and pancreas
1	B	200 nM S961	Liver and pancreas
2	A	200 nM S961	Liver and pancreas
2	B	200 nM S961	Liver and pancreas
3	A	200 nM S961 + 10 μM EdU	Liver and pancreas
3	B	200 nM S961 + 10 μM EdU	Liver and pancreas
4	A	200 nM S961 + 10 μM EdU	Liver and pancreas
4	B	200 nM S961 + 10 μM EdU	Liver and pancreas
5	A	100 nM S961	Liver and pancreas
5	B	100 nM S961	Liver and pancreas
6	A	100 nM S961	Liver and pancreas
6	B	100 nM S961	Liver and pancreas
7	A	0 nM S961	Liver and pancreas
7	B	0 nM S961	Liver and pancreas
8	A	0 nM S961	Liver and pancreas
8	B	0 nM S961	Liver and pancreas
9	A	0 nM S961 + 10 μM EdU	Liver and pancreas
9	B	0 nM S961 + 10 μM EdU	Liver and pancreas
10	A	0 nM S961 + 10 μM EdU	Liver and pancreas
10	B	0 nM S961 + 10 μM EdU	Liver and pancreas
11	A	10 nM Ex-4	Liver and pancreas
11	B	10 nM Ex-4	Liver and pancreas
12	A	10 nM Ex-4	Liver and pancreas
12	B	10 nM Ex-4	Liver and pancreas

The purpose of the third chip experiment was to perform a general functionality test of co-cultures and single cultures of liver spheroids and pancreatic islets. The experiment was conducted according to the general protocol with some exceptions. Spheroids were pooled in insulin-free chip medium and incubated overnight. Chambers were filled with 320 μL medium. 100% of the medium in the chambers was exchanged every 48 hours. 5 μM EdU was added to the chips on days 2, 4 and 6 when the medium was changed.

Table 3.5: Chip 3 experimental setup.

Chip no.	Circuit	Treatment	Cell culture
1	A	Regular chip medium	Liver and pancreas
1	B	Regular chip medium	Liver and pancreas
2	A	Regular chip medium	Liver and pancreas
2	B	Regular chip medium	Liver and pancreas
3	A	Regular chip medium	Liver only
3	B	Regular chip medium	Liver only
4	A	Regular chip medium	Liver only
4	B	Regular chip medium	Pancreas only
5	A	Regular chip medium	Pancreas only
5	B	Regular chip medium	Pancreas only

The purpose of the fourth chip experiment was to examine the insulin and glucagon re-

sponsiveness of liver spheroids. The experiment was conducted according to the general protocol with some exceptions. 5 days after seeding the liver spheroids, the aggregates were picked and pooled 40 by 40. During the 2 hour incubation in insulin-free medium, liver spheroids were placed on a wave shaker. 100 % of the media were exchanged every 24 hours. The insulin-containing media were replaced with fresh insulin-containing media during all media changes. However, glucagon was only added to the medium on days 0, 2, 4 and 6 during the media changes. On days 1, 3, and 5, the medium in these chips was replaced with regular insulin-free chip medium without any added insulin. Media samples were taken at 0 and 24 hours every day from each media change. As soon as new medium was added, 0 hour samples were taken, and the media removed during media changes were taken as 24 hour samples.

Table 3.6: Chip 4 experimental setup.

Chip no.	Circuit	Treatment	Cell culture
1	A	1000 mU/L insulin	Liver only
1	B	1000 mU/L insulin	Liver only
2	A	1000 mU/L insulin	Liver only
2	B	1000 mU/L insulin	Liver only
3	A	150 mU/L insulin	Liver only
3	B	150 mU/L insulin	Liver only
4	A	150 mU/L insulin	Liver only
4	B	150 mU/L insulin	Liver only
5	A	1000 mU/L insulin	No cells
5	B	1000 mU/L insulin	No cells
6	A	Insulin-free (IF) chip medium	Liver only
6	B	IF chip medium	Liver only
7	A	IF chip medium	Liver only
7	B	IF chip medium	Liver only
8	A	350 pM glucagon	Liver only
8	B	350 pM glucagon	Liver only
9	A	350 pM glucagon	Liver only
9	B	350 pM glucagon	Liver only
10	A	350 pM glucagon	No cells
10	B	350 pM glucagon	No cells

The purpose of the fifth chip experiment was to analyze the insulin responsiveness of liver spheroids made from either freshly thawed cells or precultured cells. The experiment was conducted according to the general protocol with some exceptions. During the 2 hour incubation in insulin-free medium, liver spheroids were placed on a wave shaker. Some of the spheroids were fixated in 4% paraformaldehyde in PBS and then stored in ethanol at 4°C until the end of the experiment. 100 % of the media were exchanged every 24 hours as described for chip 4.

Table 3.7: Chip 5 experimental setup.

Chip no.	Circuit	Treatment	Cell culture
1	A	No insulin	Precultured cells
1	B	No insulin	Precultured cells
2	A	No insulin	Precultured cells
2	B	No insulin	Precultured cells
3	A	150 mU/L insulin	Precultured cells
3	B	150 mU/L insulin	Precultured cells
4	A	150 mU/L insulin	Precultured cells
4	B	150 mU/L insulin	Precultured cells
5	A	No insulin	Freshly thawed cells
5	B	No insulin	Freshly thawed cells
6	A	No insulin	Freshly thawed cells
6	B	No insulin	Freshly thawed cells
7	A	150 mU/L insulin	Freshly thawed cells
7	B	150 mU/L insulin	Freshly thawed cells
8	A	150 mU/L insulin	Freshly thawed cells
8	B	150 mU/L insulin	Freshly thawed cells

3.3.4 Sample analysis

For chip experiments 1 and 2, media sampled during the media changes was analyzed to evaluate the level of cytotoxicity among the liver spheroids by measuring the levels of LDH in the media. The media samples taken during chip experiment 2 were also used to analyze the functionality of the liver cells by measuring the levels of albumin secreted into the medium. The spheroid samples that had been fixated and sectioned were stained with Hematoxylin and Eosin (H&E), as well as via immunohistochemistry (IHC) for the presence of CYP3A4, albumin, vimentin and α-SMA. Samples from chip experiments 4 and 5 were also stained with periodic acid staining to analyze the spheroids' abilities to store glycogen.

3.3.4.1 Cytotoxicity evaluation

On the same day as the samples were taken, the levels of LDH present in the medium was analyzed using the Pierce LDH Cytotoxicity Assay Kit. The reaction mixture for the analysis was prepared according to the manual. Media samples were diluted 1:5 in cell culture grade water, and 50 μL from each sample was transferred to a flat bottom 96-well plate in duplicates. For the blank, cell culture medium diluted 1:5 in water was used. Fifty μL reaction mixture was then added to each well containing a sample/blank, and the plate was incubated in the dark at room temperature for 30 minutes. Afterwards, the reaction was stopped by adding Stop Solution to all wells and the samples were mixed by gently tapping the plate. The absorbance at 490 nm and 680 nm (background) was measured in a spectrophotometer, after which the background values were subtracted from the 490 nm absorbance values. Since the shelf-life of the standard is very short, a standard curve was prepared and analyzed in a spectrophotometer as soon as the kit arrived. These values were then used to determine the levels of LDH present in the media from both chip experiments 1 and 2.

3.3.4.2 Albumin secretion

Samples from the second chip experiment were centrifuged at 3000 x g for 10 minutes to remove any cell debris. The concentration of secreted albumin in the media samples were analyzed using the Human Albumin ELISA kit from Abcam. Reagents including diluent, wash buffer, biotinylated albumin detector antibody, streptavidin (SP) conjugate, and albumin standard were prepared according to the manual. Samples were diluted 1:150 in diluent, and all reagents, samples and standards were allowed to equilibriate to room temperature. 50 μL of the albumin standards and samples were added in duplicates to the wells of the ELISA plate. The plate was covered with sealing tape and incubated overnight at 4 °C.

The next day, the plate was equilibriated to room temperature and washed manually according to the protocol. Fifty μL biotinylated antibody solution was added to each well and the plate was incubated at room temperature for 30 minutes. Afterwards, the plate was washed again, and 50 μL SP conjugate was added to each well. The plate was incubated for another 30 minutes at room temperature and washed again. Fifty μL chromogen solution was then added to each well, and the plate was incubated at room temperature for 20 minutes until a blue color developed. The reaction was quenched by adding stop solution to each well and the absorbance was read immediately in a spectrophotometer at 450 nm and 570 nm (background). The background values were subtracted from the absorbance values, and a standard curve was generated by regression analysis using four-parameter logistic curve-fit. The mean of the sample absorbances was calculated and the concentration of albumin present in the samples was determined from the standard curve.

3.3.4.3 Spheroid staining and immunohistochemistry

Spheroids from each chip experiment had been sent to HistoCenter for embedding in paraffin and sectioning. HistoCenter also stained sections from each experiment with H&E, and sections from experiments 3, 4 and 5 with PAS (glycogen staining). These samples were visualized under a bright-field microscope.

Table 3.8: Details of the primary and secondary antibodies used for ICC and IHC.

1° AB	Dilution	Function	2° AB	Dilution
CYP3A4	1/100	Phase I metabolizing enzyme	Alexa Fluor 488	1/400
Albumin	5 mg/mL	Plasma protein, regulates osmotic pressure	Alexa Fluor 555	1/500
Vimentin	5 mg/mL	Cytoskeletal protein	Alexa Fluor 488	1/400
α-SMA	1/50	Myofibroblast marker	Alexa Fluor 555	1/500

The remaining sections were stained with antibodies for 4 different protein markers. Samples were deparaffinzied and epitopes were retrieved by immersing the sample slides in DIVA decloaking agent in a cuvette, and placing the cuvette in a steamer for 40 minutes (20 minutes heating + 20 minutes cool down). Afterwards the slides were washed twice in Hot Rinse and then in dH_2O. The samples were placed briefly in PBS before incubating them in blocking buffer (10% BSA in PBS) for 45 minutes. Afterwards, samples

were stained with primary and secondary antibodies as described in section 3.3.1.1 for staining stellate cells. The samples on each slide were stained for two proteins. CYP3A4 was co-stained with albumin, and vimentin was co-stained with α-SMA (Table 3.8). After counterstaining with Hoechst and washing in PBS, a drop of mounting medium was placed onto each slide and a coverslip was placed on top of the sections. Slides were wrapped in aluminum foil and stored at 4 °C until visualization under a confocal microscope.

4. Results and discussion

In this chapter, data obtained from the various analyses are presented in the form of graphs and figures. The results are also evaluated and discussed.

4.1 MetID results

In this sections, results obtained from the MetID experiments using 2000 cell PHH spheroids will be presented and discussed, including results from a pilot study to determine incubation parameters, LC-MS data of the metabolite formation in PHH spheroids from AZ-compounds, and a CYP activity analysis.

4.1.1 Pilot study

Before initiating the MetID experiments, a pilot study using five commercially available substances and one internal AZ-compound was conducted. This experiment was run in order to determine the time points for sampling, the number of spheroids needed for each sampling, and whether the spheroids would show any difference in metabolism compared to previous results from hepatocyte suspension cultures. For this study, 10 PHH spheroids consisting of 2000 cells each were used for each sampling instance, and supernatants and spheroids were continually sampled during 72 hours. The 5 commercially available compounds used were benzbromarone, chlorpromazine, diclofenac, imipramine and ticlopidine. Biotransformation of the 6 compounds was investigated by analyzing the metabolites formed via LC-MS. The data obtained was compared to previous results seen both in hepatocyte suspension incubations as well as in humans during clinical trials (data not published).

The results indicated that 20 000 cells, or 10 spheroids, was enough to yield substantial levels of metabolites. The most critical sampling time points were 0, 4, 8, 24, 48 and 72 hours. Overall, certain discrepancies were seen between the spheroid data and the hepatocyte suspension data, as well as between the spheroid and human data. Various metabolites were detected in the spheroid samples for all compounds that had not been detected in the hepatocyte suspension cultures. These metabolites had, however, been detected in humans, indicating that PHH spheroids might at a certain level be able to better predict the metabolism of compounds in humans compared to PHH suspensions.

For instance diclofenac, a substrate of CYP2C9, was converted to hydroxyl-diclofenac early during the experiment (data not published). There was also evidence for glucuronosyltransferase (GT) activity as diclofenac acyl glucuronide and what might have been hydroxy diclofenac acyl glucuronide were seen. The acyl glucuronide conjugation of hydroxyl-diclofenac by the GT enzyme, has been seen to occur after the initial oxidiation of diclofenac by CYP2C9 in clinical studies [72], but not in cell suspension [73]. These results suggest the presence of sequential metabolism in the spheroids, something that

is hardly seen in suspension incubations. For the AZ-compound, there was evidence of CYP, epoxide hydrolase, glucuronosyltransferase and sulfotransferase activty, as well as glutathione conjugation (data not published). This further indicates the presence of sequential metabolism in the liver spheroids. Nevertheless, spheroids were not able to fully simulate the metabolism seen in humans for any of the compounds. For the 6 compounds included in this study, no differences between the medium and cell samples were detected.

4.1.2 Metabolite formation in PHH spheroids

Selected data from the metabolite formation of certain compounds in PHH spheroids detected by LC-MS is presented below in Tables 4.1 to 4.8. Since the compounds owned by Astra Zeneca are not officially available on the market, names and structures have been omitted. The type of metabolism seen to occur is therefore presented in the first column of the tables below. The cells for the corresponding systems (human *in vivo*, PHH suspension or PHH spheroids) where the individual metabolites were seen have been colored green. PHH suspensions are normally incubated with a compound for 4 hours. Spheroids were incubated with the compounds for 72 hours.

Table 4.1: Metabolism of AZD1.

Metabolism	*In vivo*	PHH suspension	PHH spheroids
Hydroxylation			
Amide hydrolysis			
Ring opening			
Oxidation			
Demethylation			
Glucoronidation			
Sulfation			
Conjugation of oxygen			

Table 4.2: Metabolism of AZD8.

Metabolism	*In vivo*	PHH suspension	PHH spheroids
Oxidation			
Glucoronidation			
Carboxylation			
Hydroxylation			
Sulfation			
Methoxylation			

Table 4.3: Metabolism of AZD9.

Metabolism	*In vivo*	PHH suspension	PHH spheroids
Hydroxylation			
Glucoronidation			
Oxiadation			
Dealkylation			
Chain shortening			
Conjugation of oxygen			

Table 4.4: Metabolism of AZD11.

Metabolism	*In vivo*	PHH suspension	PHH spheroids
Amide hydrolysis			
Dealkylation			
Glucoronidation			
Demethylation			
Oxidation			
Hydroxylation			

Table 4.5: Metabolism of AZD15.

Metabolism	*In vivo*	PHH suspension	PHH spheroids
Dealkylation			
Glucoronidation			
Desulfation			
Methylation			
Hydroxylation			
Conjugation of oxygen			
Reduction			

Table 4.6: Metabolism of AZD16. No data was found for microsomes or PHH suspensions.

Metabolism	*In vivo*	Microsomes/ PHH suspension	PHH spheroids
Glucoronidation			
Sulfation			
Demethylation			
Hydroxylation			
Amide hydroxylation			
Methylation			
Ring deethylation			
Dealkylation			

Table 4.7: Metabolism of AZD17.

Metabolism	*In vivo*	PHH suspension	PHH spheroids
Ring deethylation			
Glucoronidation			
Hydroxylation			
Uncommon metabolites		Fewer than *in vivo*	Fewer than *in vivo*
Dealkylation			
Methylation			
Oxidation			
Conjugation of nitrogen			
Conjugation of oxygen			

Table 4.8: Metabolism of AZD23.

Metabolism	*In vivo*	Microsomes/ PHH suspension	PHH spheroids
Hydroxylation			
Oxidation			
Glucoronidation			
Nucleophilic aromatic substitution		Microsomes only	Defluorination
Sulfation			
Conjugation of oxygen			

Of all the compounds tested in the PHH spheroids, not all had any PHH suspension data available. Also, some compounds were either unstable in DMSO at room temperature or contained impurities prior to the experiments. Data from these compounds have therefore not been published in this thesis. As can be seen from the tables above, there is not a perfect overlap in the metabolism seen between either the spheroids and humans, or the suspension cultures and humans. CYP activity was prominent in the spheroids, since all compounds that were hydroxylated in humans were also hydroxylated in the spheroids, unlike the PHH suspensions (Tables 4.1 and 4.7). For some compounds, secondary metabolism seen in humans, but not the suspension cultures, was also present in the spheroids, such as some of the glucoronidations. Overall for all compounds though, more metabolites variations of the same type of biotransformation were found *in vivo*. For instance, some compounds were glucuronidated on various different sites on the molecules in vivo, whereas the same compounds were glucuronidated on only one or two sites on the molecules in the spheroids and in PHH suspensions (data not shown).

The overlap between human metabolism and PHH spheroids was not as large as expected. In these experiments, spheroids did not prove to be a significantly better model for investigating the metabolism of compounds *in vitro* compared to suspension cultures. This could be due to a number of reasons. The medium used during the incubation of the MetID compounds was not optimized for long-term cultivation of the hepatocytes, and might have affected their metabolic functions negatively. While hepatocytes are the major metabolizing cells in the liver, incorporation of other cells into the spheroids might also have an effect on the overall metabolism. In humans, other other organs capable of metabolizing xenobiotics and other substances are present, such as the kidneys. Co-cultures of different organ models might thereby increase the similarities between *in vivo* and *in vitro* metabolism. Also, some of the compounds such as AZD8 and AZD9 (Tables 4.2 and 4.3) were small and polar. This shortens the retention time of the metabolites on the column, and any eluted compounds are difficult to separate. Other methods should therefore be used to separate the metabolites formed from these compounds.

It should also be noted that this has been a qualitative comparison between quantitative in vivo data from human plasma with radiolabeled drugs and data from PHH spheroids incubated with unlabeled compounds. This type of analysis is therefore only valid to investigate whether the metabolism seen in humans occurred in spheroids or not, but to compare the levels of metabolites formed in humans and PHH spheroids, quantitative analysis of spheroid metabolism needs to be conducted. To be able to rule out any metabolic varieties between different donors, compounds should also be tested in spheroids and suspensions of cells from the same donor and batch. Overall, spheroids are probably

a promising substitute for suspension cultures in MetID analyses, since they are capable of both primary and secondary metabolism and can be maintained in cultures for longer periods of time. For any future studies, however, parameters such as medium composition need to be optimized to be able to conclude whether spheroids are able to better mimic human metabolism *in vivo* compared to suspension cultures.

4.1.3 CYP1A2, 2C9, 2D6 and 3A4 enzyme activity

Along one of the MetID experiments, the activity of CYP1A2, 2C9, 2D6 and 3A4 in the same batch of PHH was followed over the course of 10 days. Spheroids were incubated with one substrate for each enzyme, and the concentration of each corresponding metabolite formed was measured. Figure 4.1 illustrate the enzyme activity of the four CYPs on three instances over the 10 days. On day 0, when the cells were thawed, cells in suspension were incubated with the four CYP substrates. On days 7 and 10, 2000 cell spheroids where pooled and incubated with the substrates. As can be seen in the figure, between days 0 and 7, the activities of CYP1A2 and 2D6 decline as the levels of paracetamol and 1'-OH-bufuralol formed decreases. In the same time span, the activity of CYP3A4 increases as the levels of 1'-OH-midazolam formed increases, while the activity of CYP2C9 remains stable. However, between days 7 and 10, the activities of all CYPs decrease significantly.

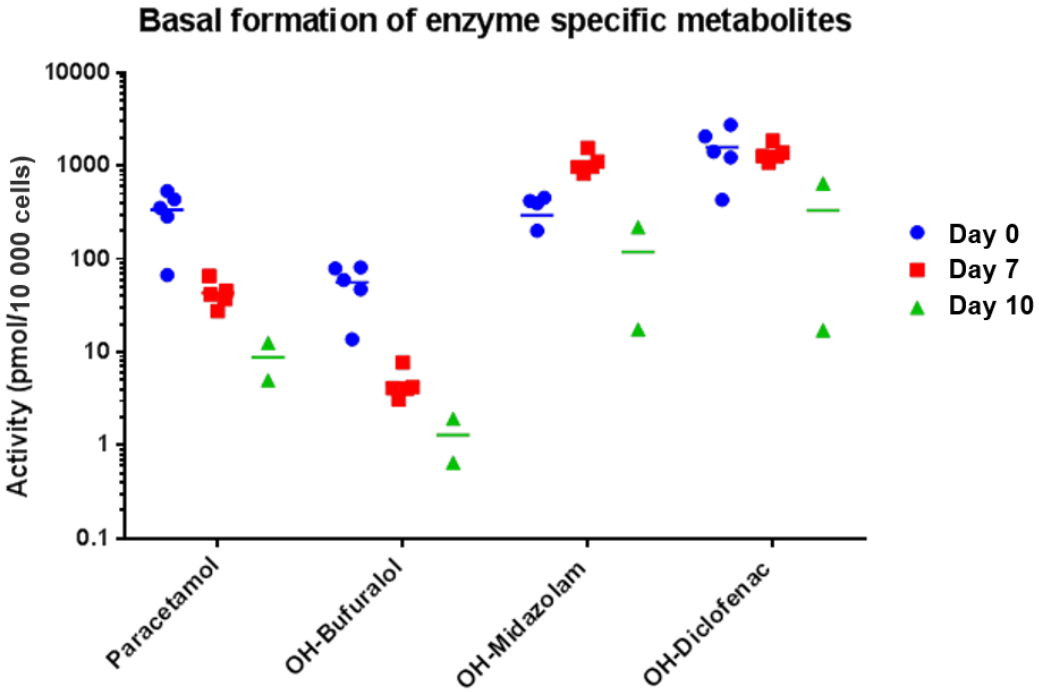

Figure 4.1: Enzyme activity of CYP1A2, 2D6, 2C9 and 3A4 over the course of 10 days. CYP1A2 metabolizes phenacitin into paracetamol, 2D6 metabolizes bufuralol into OH-bufuralol, 2C9 metabolizes diclofenac into OH-diclofenac, and 3A4 metabolizes midazolam into OH-midazolam. On day 0, CYP activity was measured in cells in suspension, on days 7 and 10 CYP activity was measured in spheroids formed from the same batch of cells.

During the first 7 days, cells were seeded and cultured in complex media (PHH seeding and culturing media, Table 3.1). The seeding medium contains 10% serum (FBS), which is quite high, and this might have affected the activities of CYPs 1A2 and 2D6. Previous

studies have shown that high serum concentrations (>1%) lead to a significant decrease in CYP1A activity [74]. However, when maintained in PHH culturing medium, the activities of all 4 CYPs remain stable in PHH spheroids over the course of 35 days [8]. At the start of the MetID experiment on day 7, the culturing medium was exchanged for MetID incubation medium. The spheroids used for the CYP activity were therefore also cultured in the same type of medium (without any added MetID-specific compounds) for the remaining 3 days.

Since the drop in activity for all CYPs investigated is large over the last 3 days, especially for CYPs 3A4 and 2C9 compared to the first 7 days in PHH culturing medium, the most likely explanation to this behavior is the medium change. The PHH medium is more complex than the MetID incubation medium which, based on current results, is not sufficient for the spheroids to survivie for longer culture times. However, even though the medium was changed, some activity was still detected, and positive results were obtained from the MetID experiments as well. Nevertheless, since the MetID incubation medium seems to have affected the CYP activity in the spheroids negatively, other enzymes involved in the metabolism of the compounds used in the MetID experiments might have been affected as well. If cultured in PHH culturing medium throughout the entire experiment, the outcome may have been different, which is something that should be investigated in the future.

4.2 Chip results

In this section, results from the chip experiments using 25 000 cell HepaRG/stellate cell spheroids will be presented and discussed, including results from stellate cell culturing, LDH and albumin analyses, and stainings of the spheroids used in the 2-organ chips.

4.2.1 Stellate cell culturing and staining

During the chip experiments, cryopreserved primary human stellate cells were cultured in cell culture flasks in order to develop a protocol for preculturing the cells before seeding them with HepaRG cells into spheroids. By preculturing cells, non-viable cells are effectively removed, improving the viability and quality of cells in co-culture spheroids. Preculturing stellate cells is also an efficient way of activating the cells, which have been shown to aid the formation of spheroids [47]. During the first attempt, stellate cells were cultured in non-treated cell culture flasks and PLL-coated cell culture flasks. Two different types of media were initially used, one for hepatic cells in general (PHH thawing medium, Table 3.1) and one specifically developed for stellate cells (HSGM). Since the cells were not able to proliferate in the general medium, this medium was not used for later analysis.

When viewed under a bright-field microscope, cells appeared to grow in patches in both types of flasks rather than over the entire surface. However, while cells in the non-treated flasks appeared small and striated (Figure 4.2), cells in the PLL-cultured flasks were able to extend cell membrane protrusion and cover a larger surface area of the flasks (Figure 4.3). When subculturing the cells, it also became apparent that cells cultured in the PLL-coated flasks were able to increase in number more efficiently than the cells cultured in non-treated flasks. Stellate cells also seemed to rely a lot on being in close contact with other cells to be able to proliferate, since any cells that were not in close enough contact with the more dense patches quickly died. Also, rather than extending further over the

surface of the flasks, the patches quickly became overconfluent. This instigated the cells to start excreting extensive amounts of extracellular matrix proteins, which formed a large sheet around the cells that was near impossible to break apart, neither enzymatically nor with physical force. These results indicate that it is important to initially seed cells at a high density, and to rather subculture the cells at a lower confluency to avoid overconfluency.

Cells cultured in the two types of flasks were also immunofluorescently stained for vimentin, a cytoskeletal protein found in human stellate cells, and α-SMA, a myofibroblast marker which would indicate whether the cells were starting to differentiate. When activated, stellate cells are able to proliferate and increase in number, but there is also a risk that they might differentiate into myofibroblasts. As seen in Figure 4.2, a lot of α-SMA is present, indicating that the cells are indeed differentiating into myofibroblasts when cultured on a non-treated surface. Cells cultured on PLL on the other hand (Figure 4.3) are expressing lower levels of α-SMA, but are rather spreading over the surface with long processes. This indicates that culturing cells in stellate cell-specific medium on a PLL-coated surface might improve their ability to maintain an activated and proliferative phenotype without differentiating into myofibroblasts.

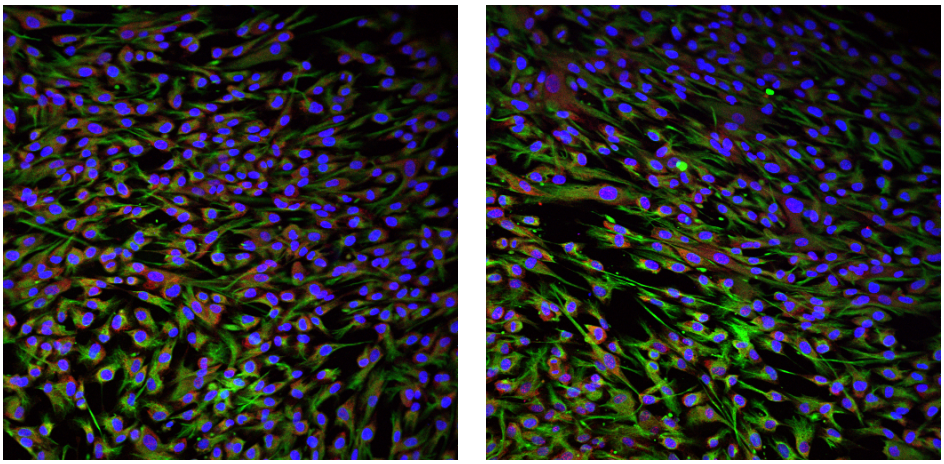

Figure 4.2: Stellate cells cultured in non-treated cell culture flasks, stained for vimentin (green) and α-SMA (red). Cell nuclei appear in blue. Images taken at 40X magnification.

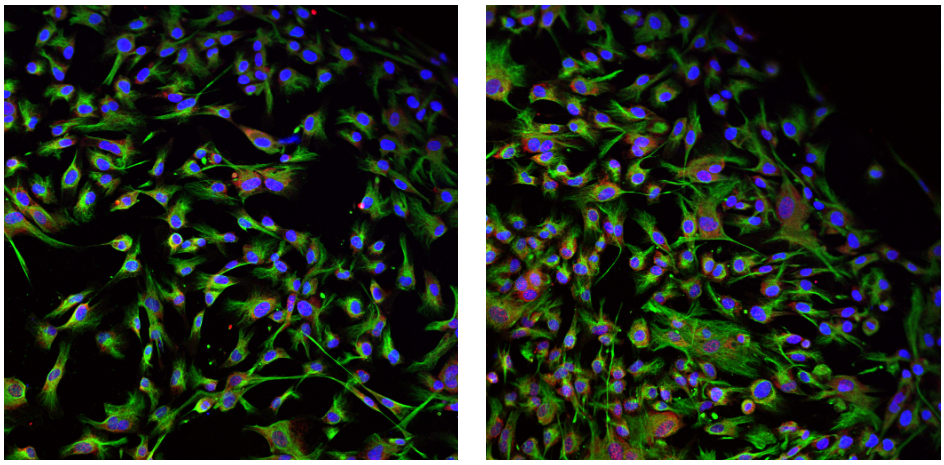

Figure 4.3: Stellate cells cultured in PLL-coated cell culture flasks, stained for vimentin (green) and α-SMA (red). Cell nuclei appear in blue. Images taken at 40X magnification.

During the second attempt, stellate cells were cultured in stellate cells medium (Table 3.1) in tissue culture-treated flasks. The new stellate cell medium was used since it has been shown to be effective when culturing stellate cells [14][12]. The tissue culture-treated flasks were used to investigate whether they could replace the PLL-coated flasks, which would reduce cost as well as labor intensity, since these flasks did not need to be manually coated.

After thawing the cells, they were seeded at a density more than 3 times higher than during the first attempt. This proved to be beneficial as the cells were able to properly coat the surface of the flask and start proliferating. Cells were also subcultured at a confluency of no more than 80%, and after the first passage, cells could be seeded into new flasks at a lower cell density. After 1-2 passages, cells started to expand rapidly and needed to be subcultured more often, indicating that all cells were properly activated. Stellate cells of passage 4 were later used to form spheroids with HepaRG cells for a chip experiment, and spheroids were stained before and after being used in the chips (Section 4.2.4.4). As the cells were able to grow and expand easily and were successfully incorporated into co-culture spheroids with HepaRG cells, the new stellate cell culturing protocol was deemed successful.

4.2.2 Cytotoxicity of liver spheroids in 2-organ chips

To evaluate the systemic viability of the co-cultures in the 2-organ chips, the levels of LDH in the chip medium were measured during chip experiments 1 and 2. LDH, or lactate dehydrogenase, is a cytosolic enzyme present in the hepatic cells catalyzing the conversion of L-lactate and NAD to pyruvate and NADH during glycolysis [14]. When the plasma membranes of the cells are damaged, LDH is released into the surrounding medium.

As can be seen in Figure 4.4, the LDH levels from the first chip experiment are initially very high and steadily decreasing up until day 7, except for in the liver only circuit where the LDH levels remain high until day 4 before decreasing. Since the HepaRG cells are immortalized cells, they might express higher levels of LDH compared to PHH [75]. However, for this experiment, the initial concentrations of LDH are almost 10 times as high compared to previous studies performed in multi-organ chips [13][14][15]. This probably results from spheroids disintegrating early in the experiment. Figure 4.5 presents a rep-

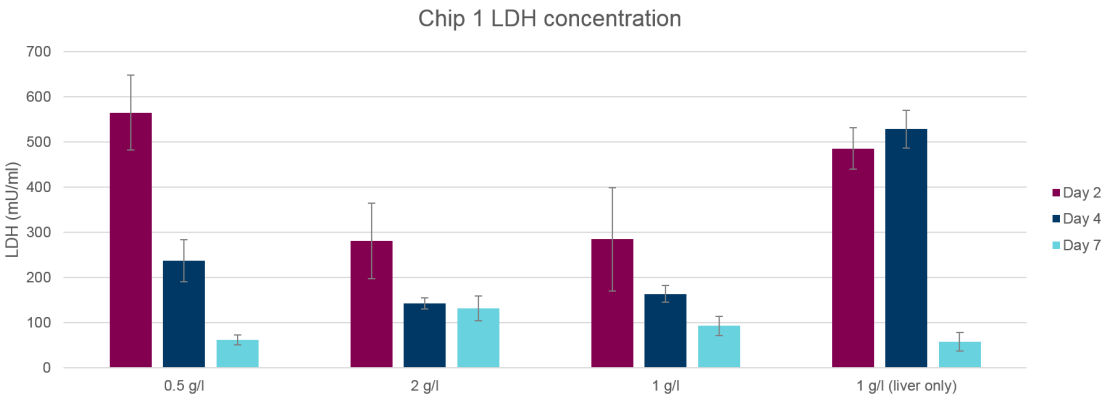

Figure 4.4: Cytotoxicity assessment of the liver spheroids used in the first chip experiment. The vertical axis presents the LDH concentration in mU/mL, the horizontal axis presents the different groups from the media tests (the different glucose concentrations) sampled during days 2, 4 and 7

resentation of the spheroids while in the 2-organ chips during the first and second chip experiments. The images clearly show disrupted spheroids and cell debris, which would lead to the release of large quantities of LDH into the chip medium.

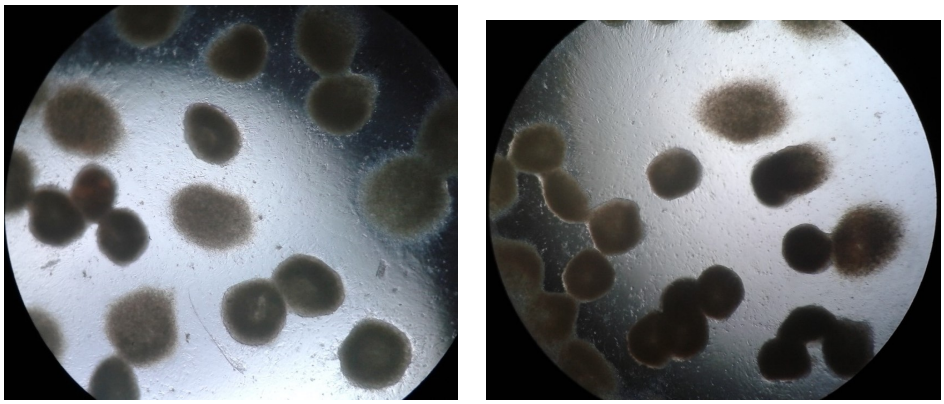

Figure 4.5: Live images of liver spheroids in the 2-organ chips. Some of the spheroids appear to be disintegrating while others remain intact. A hollow core can also be seen in a few of the spheriods. Images taken at 5X magnification.

On day 1 during the second chip experiment, the concentration of LDH averaged around 50 mU/mL for all different settings (Figure 4.6). These results are consistent with previous studies, which found that the artificial culturing conditions and shear stress might initially lead to an increased cell turnover rate [13][15]. However, unlike previous findings where the conditions and cell turnover rate stabilized over time, LDH levels for the second chip expeirment continued to rise. On day 7, the concentration of LDH started to decrease again.

The decreasing levels of LDH seen towards the end of the experiments is likely due to many spheroids having disintegrated by the end of the experiments. For the first chip experiment, co-cultures of livers and islets incubated in chip medium with either 1 g/L or 2 g/L glucose

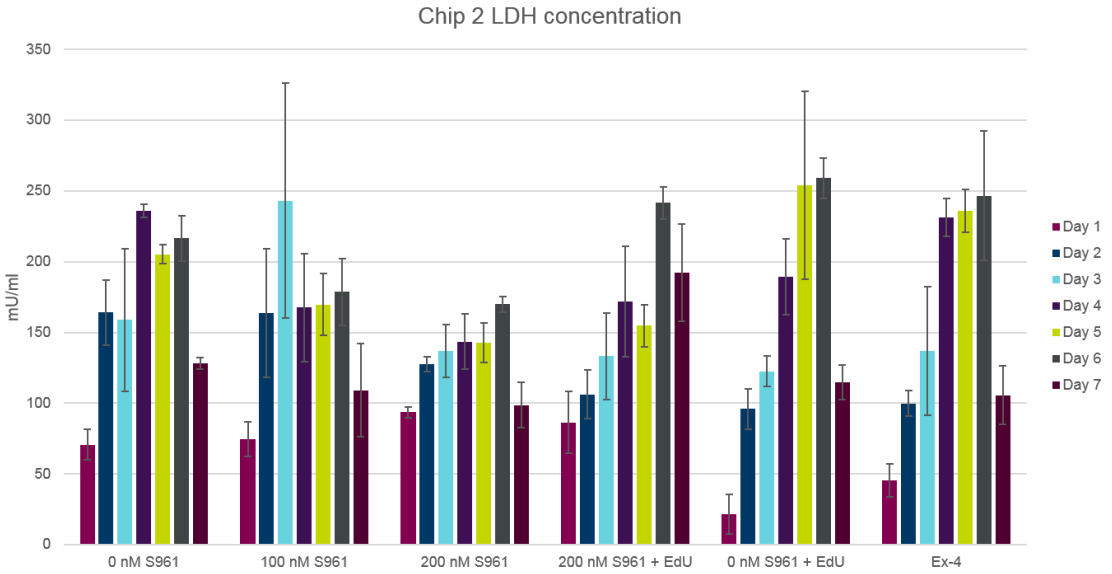

Figure 4.6: Cytotoxicity assessment of the liver spheroids used in the second chip experiment. The vertical axis presents the LDH concentration in mU/mL, the horizontal axis presents the different groups sampled during days 1 through 7

initially appeared to be more viable compared to co-cultures in 0.5 g/L glucose, since the concentrations of LDH in these cultures on day 2 were significantly lower than those in the 0.5 g/L glucose medium. However, since the concentration of LDH was elevated for all conditions during the two experiments, it is difficult to tell whether the different media and peptide concentrations had significantly different effects on cell viability. A possible explanation for the increased release of LDH could be that the spheroids used for these two experiments were made entirely from freshly thawed cryopreserved cells rather than precultured cells. This can lead to a higher incorporation of damaged or non-viable cells in the spheroids, which could trigger apoptosis or necrosis in the surrounding cells. The large size of the spheroids (25 000 cells) might also lead to insufficient diffusion of nutrients to the inner cells, which could also trigger apoptosis in the spheroids. Another possible explanation for the disintegration of spheroids might be increased shear stress from the circulating fluid. There were some issues with one of the pumps used during the first chip experiments, which lead to increased pressure in the units. This pump was later replaced for the final chip experiments.

4.2.3 Secretion of synthesized albumin

As a way to monitor liver-like activity in the 2-organ chip co-cultures, the levels of secreted albumin synthesized by the liver spheroids were measured during the second chip experiment. On day 1, the amount of albumin secreted into the medium averaged around 7 μg/mL/circuit (Figure 4.7), except for the cultures incubated with Ex-4 (a GLP-1 receptor agonist), which correlates well with previous studies conducted on HepaRG cells [12][76]. On day 4 of the experiment, the albumin present in the medium seems to have increased for most conditions. Since only 50% of the medium had been exchanged every 24 hours between days 1 and 4, albumin secreted between these time points might have accumulated slightly, which could explain the increase in albumin concentration. Also, as indicated above for the release of LDH into the medium, cells were suffering from decreasing viability. The lysis of cells could have caused release of intracellular storages of

albumin as well.

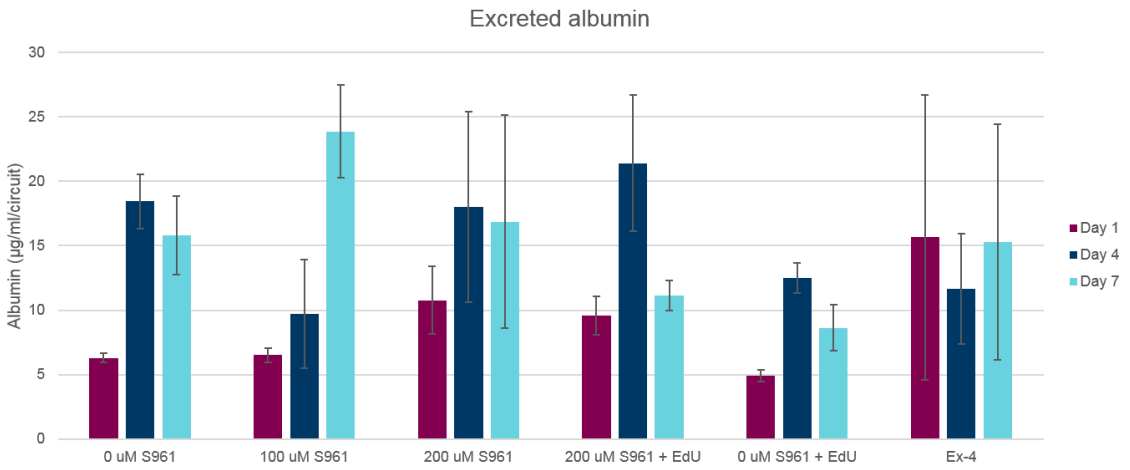

Figure 4.7: Excreted albumin synthesized by liver spheroids during the second chip experiment. The vertical axis represents the albumin concentration in μg/mL/circuit and the horizontal axis represents the different co-culture conditions. The colors of the bars represent the time points when the samples were taken.

On day 6, 100% of the medium was exchanged. The samples taken on day 7 had therefore been incubated in chip medium for the same amount of time as the samples taken on day 1. The samples taken from the co-cultures incubated with S961 without EdU were all elevated compared to day 1, while the samples from the remaining three conditions were almost the same as on day 1. This indicates that while cells were dying during the experiment, spheroids were still functional and able to display liver-like activity somewhat consistent to previous studies throughout the experiment for all conditions tested.

4.2.4 H&E, PAS and immunofluorescent stainings of liver spheroids

After finishing all chip experiments spheroids were collected and stained using several different assays. Spheroids from all experiments were stained with H&E as well as for 4 different protein markers via IF staining. The glycogen storages in spheroids from chip experiments 3, 4 and 5 were stained via PAS as well.

4.2.4.1 H&E

H&E color the nuclei of the cells and cytoplasmic components respectively. While hematoxylin develops a dark blue or purple color, eosin appears in red and pink hues. Figure 4.8 presents images of spheroids stained with H&E from different chip experiments and conditions that visually represent the majority of all spheroids from all chip experiments. Many of the spheroids from all chip experiments and conditions displayed an almost "doughnut-like" shape with a hollow core. This structure might be due to spheroids forming a cavity similar to a central vein (Figure 2.2). In future experiment, it might therefore be of interest to include endothelial cells in the spheroids and investigate whether they line this type of cavity, which would be a sign that the spheroids are actively trying to form parts of a vascular system. It might also be a prominent example of the formation of a necrotic core. Since the spheroids are completely avascular, they are analogous to other similar tissues, such as tumors, with diffusion limitations of about 150-200 μm in regard

to many molecules, including oxygen [77][78]. This inefficient mass transport also leads to metabolic waste accumulation inside the spheroids. Spheroids with a size above 500 μm in diameter, much like the spheroids used in the chip experiments, have been shown to display a layer-like structure with a necrotic core surrounded by a viable rim [78]. This is clearly illustrated in the images in Figure 4.8 (especially the top left and bottom left images) were the hollow core and outer rim of the spheroid sections have a higher density of cell nuclei.

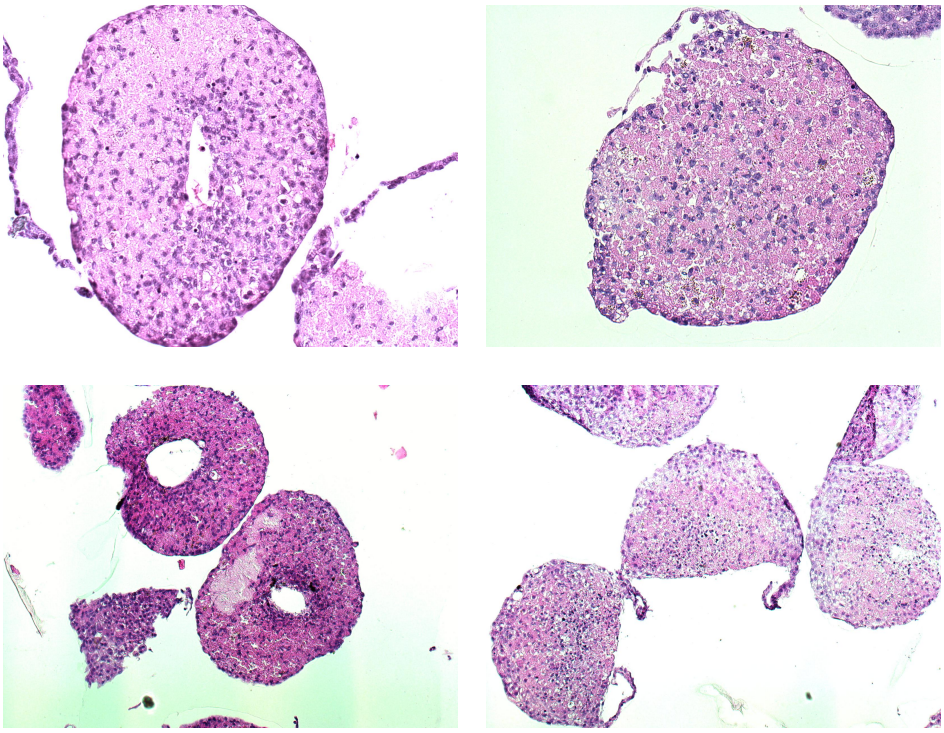

Figure 4.8: Spheroids from different chip experiments stained with H&E. **Top left**: Chip 1, 2g/L glucose medium; **Top right**: Chip 4, liver only culture treated with glucagon; **Bottom left**: Chip 6, spheroids from freshly thawed cells, incubated with regular chip medium; **Bottom right**: Chip 6, spheroids from precultured cells treated with insulin. All images were taken at a 20X magnification, except the images from chip 6, which were taken at a 10X magnification.

As can be seen in all images, there are also cytoplasmic areas inside the spheroids that completely lack cell nuclei, so called ghost cells, indicating that the cells in these areas have died. In addition, some of the images do not display a hollow core at all, but since these appear smaller in size it can be speculated that these sections do not originate from the middle of the spheroids but rather the top or bottom, where the diffusion rate of oxygen and nutrients is higher.

During chip experiment 6, some spheroids were fixated and sectioned before the initiation of the experiment. Figure 4.9 shows one image each for the two types of spheroids used. The spheroids made from freshly thawed cells were already starting to show signs of the formation of necrotic cores and ghost cells, as can be seen in the corresponding image. While the spheroids made from precultured cells appeared healthier, probably due to a higher initial cell viability, these do also start to show signs of the formation of ghost cells in certain areas, clearly indicating that the large spheroid size is indeed a problem.

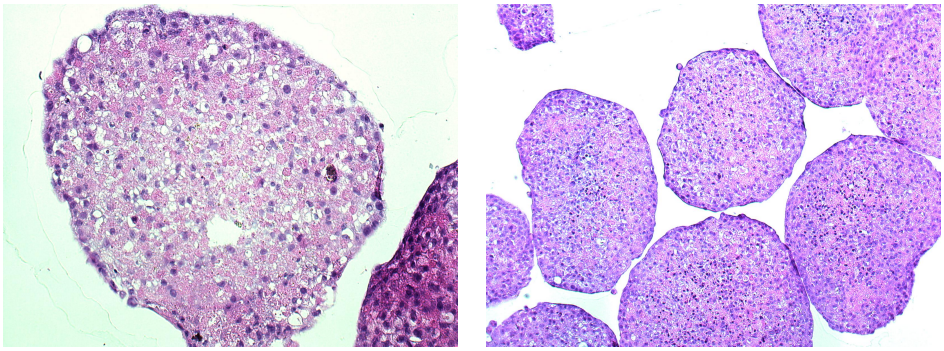

Figure 4.9: Spheroids from chip experiment 6 stained with H&E, prior to seeding spheroids into the chips. **Left**: Spheroids made from freshly thawed cells. Image taken at 20X magnification. **Right**: Spheroids made from precultured cells. Image taken at 10X magnification.

Despite being incubated in a microfluidic environment, spheroids are clearly too large for proper mass transport to occur through the spheroids. To ensure that appropriate oxygen and nutrient diffusion can take place in the spheroids, spheroid size needs to be decreased drastically. Otherwise, some form of vascularization within the spheroids needs to be constructed.

4.2.4.2 Periodic acid-Schiff stain

PAS is a type of assay used to detect polysaccharides, such as glycogen, but also glycoproteins and glycolipids, in tissues. It is useful as an aid in the diagnosis of glycogen storage disease. Upon staining, glycogen storages will appear in a dark magenta color. PAS is often used together with hematoxylin, which will stain cell nuclei in a dark blue or purple color.

In the human body, the pancreas is responsible for the secretion of insulin and glucagon, which regulate the hepatic glucose metabolism and production depending on the blood glucose concentration [79]. Insulin acts by stimulating glycogen storage in the hepatocytes and inhibits glucose production through glycogenolysis. Glucagon on the other hand is a positive regulator of hepatic glucose production, and opposes insulin actions by inducing the hepatocytes to convert glycogen storages into glucose. Abnormal levels of glucagon can cause a depletion of the liver's glycogen storages. It is therefore important to monitor the maintenance of glycogen in the liver spheroids.

Figure 4.10 presents images of spheroids stained by PAS from different chip experiments and conditions that visually represent the majority of all spheroids from all chip experiments. As can be seen from these images, all spheroids appear to have been able to maintain some glycogen storages, as seen by the areas in magenta . Since no major difference can be seen from different conditions, such as co-cultures with pancreatic islets, or addition of insulin or glucagon to the medium, neither of these conditions appear to deplete nor significantly increase glycogen storages.

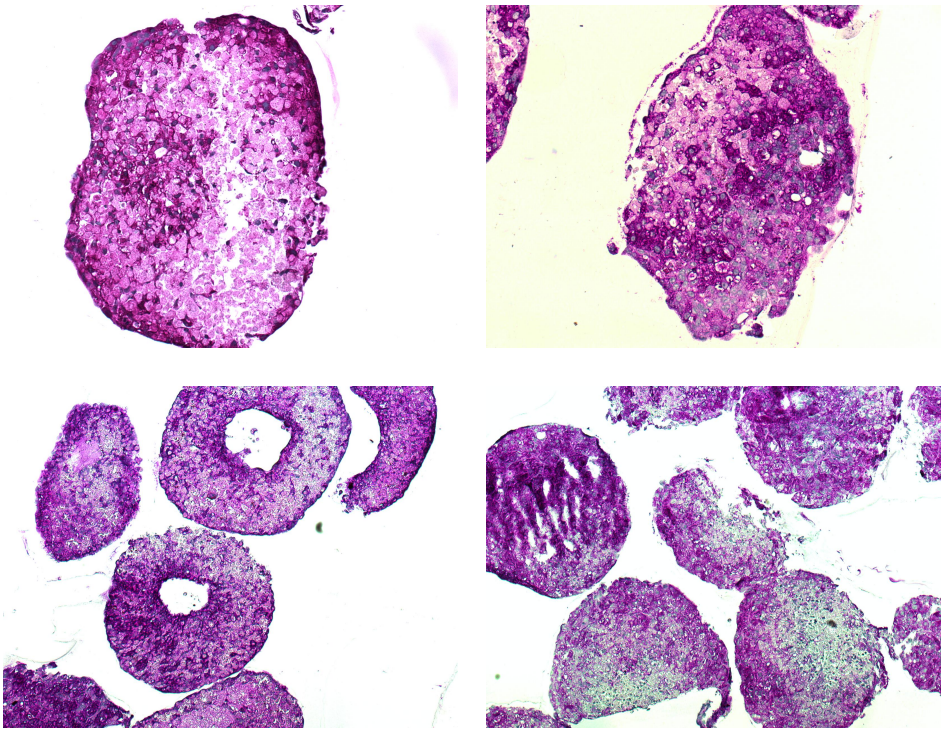

Figure 4.10: PAS staining of spheroids from different chip experiment. **Top left**: Chip 3, liver-pancreas co-culture; **Top right**: Chip 4, liver only culture treated with glucagon; **Bottom left**: Chip 5, freshly thawed cells in regular chip medium; **Bottom right**: Chip 5, precultured cells treated with insulin (low concentration). Top pictures were taken at a 20X magnification, bottom pictures were taken at a 10X magnification.

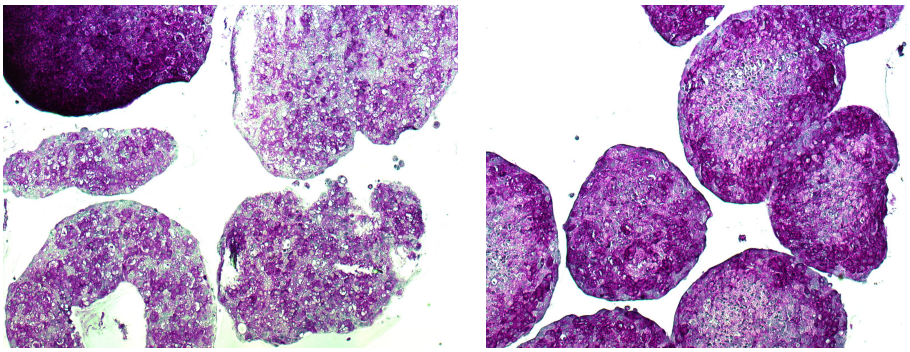

Figure 4.11: PAS staining of spheroids from chip experiment 6 prior to seeding spheroids into the chips. **Left**: Spheroids made from freshly thawed cells. **Right**: Spheroids made from precultured cells. Images were taken at 10X magnification.

Figure 4.11 presents one image each of the two types of spheroids used in chip experiment 6 that were sectioned and stained prior to seeding spheroids into the chips. While the precultured cells seem to prefer to store glycogen closer to the edges of the spheroids rather than the center, this might also be the result of the formation of a necrotic core and not storage location preference. Nevertheless, since PAS staining is a qualitative rather than quantitative assay, staining images will only provide an indication whether conditions are highly affecting glycogen storages in any way. A quantitative assay will be

able to provide a more detailed view of the differences in glycogen levels between different conditions.

4.2.4.3 CYP3A4 and albumin

Albumin, one of the most abundant blood plasma proteins produced by the liver, and CYP3A4, one of the major metabolizing enzymes in the liver, are both markers of normal liver function. Figure 4.12 shows images from different chip experiments and conditions visually representing most spheroids from all experiments.

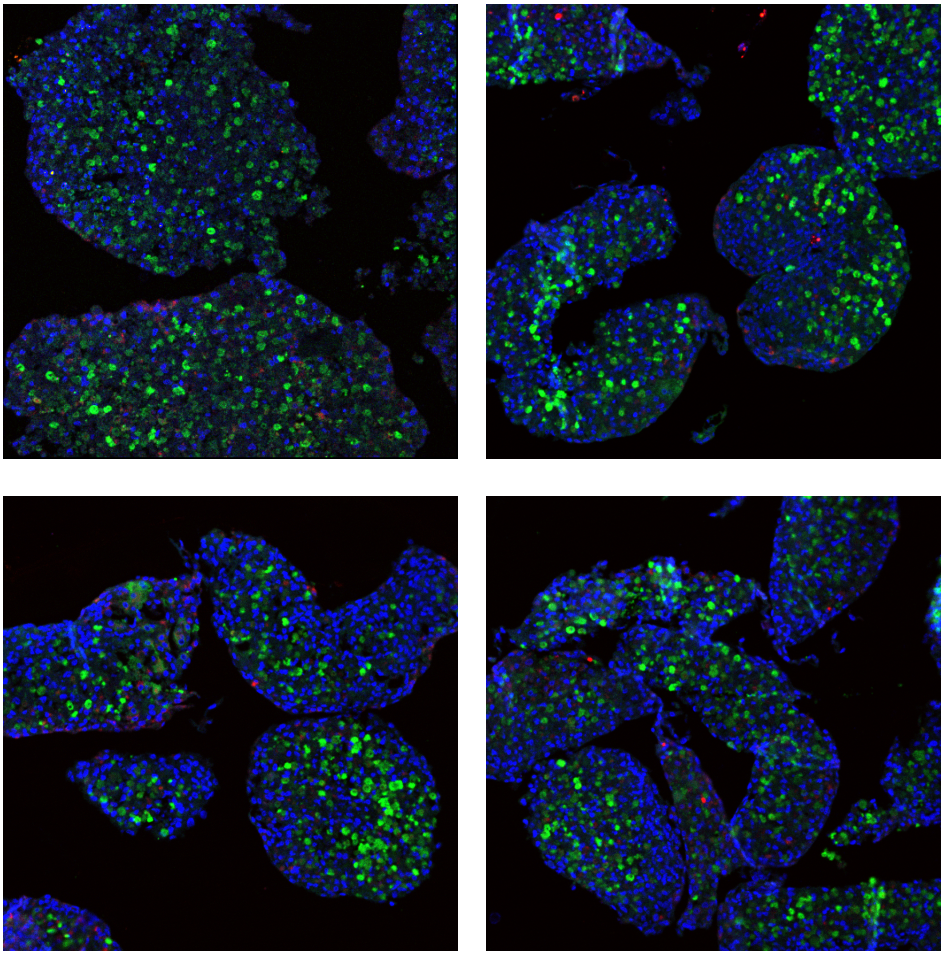

Figure 4.12: Spheroids from different chip experiments and conditions stained for albumin (red) and CYP3A4 (green). Cell nuclei are stained with Hoechst (blue). **Top left**: Chip 3, liver only culture; **Top right**: Chip 2, spheroids incubated in regular chip medium with EdU; **Bottom left**: Chip 2, spheroids incubated with 200 nM S961; **Bottom right**: Chip 2, spheroids incubated with EdU and 200 nM S961. Images taken at 20X magnification.

As can be seen from all images, CYP3A4 is expressed in large amounts in all spheroids. Some albumin can also been seen in most spheroids. Interestingly, albumin is mostly expressed around the outer edges of the spheroids, while CYP3A4, although present in most parts of the tissues, is expressed closer to the middle of the spheroids. These results correspond to the functions of a human liver, where albumin is expressed periportally and CYP3A4 is mainly expressed periveinously [2]. This shows that cells in the spheroids are

able to gain a certain phenotype depending on their physical location within the spheroids. The reason why CYP3A4 is produced throughout the spheroids might be due to the lack of diffusion within the spheroids, leading to a more periveinous-like environment closer to the surface of the spheroids compared to a human liver.

4.2.4.4 Vimentin and α-SMA

Spheroids were also stained for vimentin, a cytoskeletal protein expressed by stellate cells, and α-SMA, a protein expressed by myofibroblasts, in order to localize the stellate cells and evaluate whether they seemed to be proliferating or differentiating into myofibroblasts. Figure 4.13 shows images from different chip experiments and conditions visually representing most spheroids from all experiments. As can be seen from the images the stellate cells can easily be located by staining them for vimentin, and the lack of α-SMA indicates that they have not started to differentiate into myofibroblasts. Also, the fact that most stellate cells are located towards the middle of the spheroids rather than aroudn the edges indicate that they appear to be intercalated between the hepatcoytes, much like in the human liver [2]. For most experiments and conditions, stellate cells did not seem to proliferate. However, during chip experiment 4, as can be seen in the bottom left image, stellate cells appeared to have increased significantly in number in some conditions compared to other experiments. Stellate cells had also lined the necrotic core of certain spheroids, as seen in the bottom right image, something that was not observed during any other experiments.

During chip experiment 4, the type of culturing plates used when forming the spheroids was changed. For this experiment, spheroids were cultured in 384-well plates rather than 96-well plates. The switch to new plates initially led to the formation of slightly irregular aggregates rather than round spheroids, which might be the cause as to why stellate cells became activated and started to proliferate. For chip experiment 5, however, the protocol for culturing spheroids in 384-well plates had been improved, and increased stellate cell proliferation was not observed. The consistency in appearance and expression of α-SMA indicates that the different conditions (for instance co-culture with pancreatic islets, or addition of glucagon or S961 to the medium), does not significantly affect the viability or phenotype of the stellate cells.

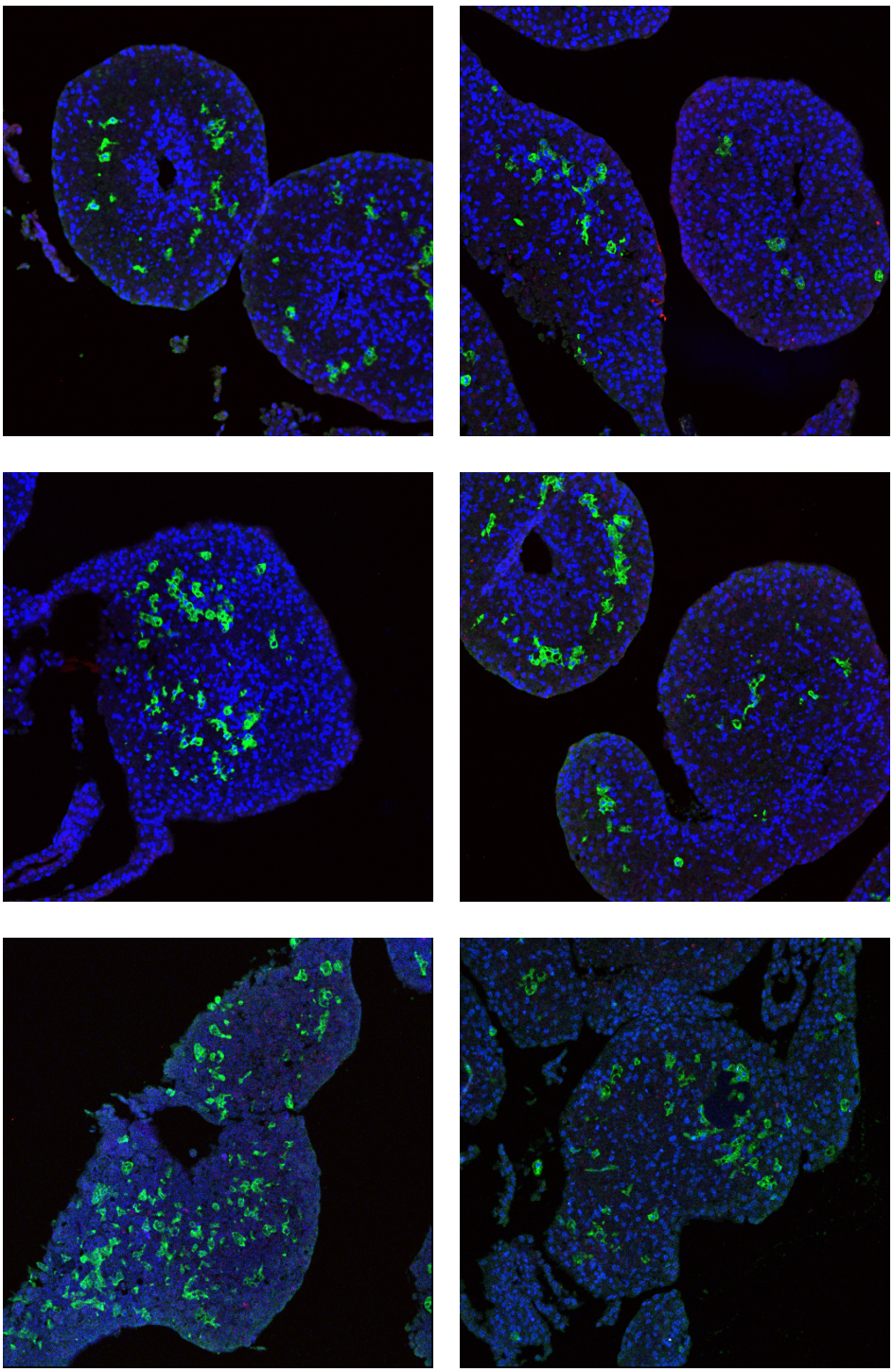

Figure 4.13: Spheroids from different chip experiments and conditions stained for vimentin (green) and α-SMA (red). Cell nuclei are stained with Hoechst (blue). **Top left**: Chip 1, spheroids incubated in chip medium with 0.5 g/l glucose ; **Top right**: Chip 1, spheroids incubated in chip medium with 1 g/l glucose; **Middle left**: Chip 1, spheroids incubated in chip medium with 2 g/l glucose; **Middle right**: Chip 1, liver only culture in chip medium with 2 g/l glucose; **Bottom left**: Chip 4, spheroids treated with glucagon; **Bottom right**: Chip 4, spheroids treated with insulin. Images taken at 20X magnification.

5. Conclusion

This thesis has had two focal points. One regarding the characterization of the formation of metabolites from a certain set of compounds in primary human hepatocyte spheroids. The other regarding the establishment and characterization of a co-culture between human liver spheroids, made from HepaRG cells and primary hepatic stellate cells, and primary human pancreatic islets in microfluidic 2-organ-chips, as well as the development of a protocol for preculturing the stellate cells used in the spheroids.

PHH spheroids were successfully seeded into spheroids and incubated with a set of different compounds. Qualitative LC-MS analysis showed that some of the metabolism seen in humans did also occur in the spheroids, however, there was not a perfect overlap between the two data sets. The use of PHH spheroids did not significantly improve the prediction of human metabolism compared to suspension cultures. Activity analysis of CYP1A2, 2D6, 2C9 and 3A4 indicated that a change of medium before the start of the experiments might have negatively affected the overall metabolic capacity of the spheroids.

Stellate cells were successfully precultured and incorporated into spheroids together with HepaRG cells. Co-cultures of the liver spheroids and pancreatic islets were maintained for 7 days in the microfluidic multi-organ chip devices. Spheroids successfully displayed some liver-like activity by synthesizing and secreting albumin at levels corresponding to previous studies on the same type of cells. Cells in the spheroids also started to develop different phenotypes depending on their physical location within the aggregates, as seen from staining sections of the spheroids for albumin and CYP3A4. PAS stainings of the liver spheroids confirmed that the spheroids were able to maintain glycogen storages throughout the entire culturing process in the chips, during both liver only-cultures as well as co-cultures with pancreatic islets. Stainings of spheroid sections for vimentin and α-SMA showed that stellate cells were easily detectable and neither proliferating nor differentiating into myofibroblast. However, H&E stainings as well as measurements of LDH levels in the culture medium indicated that cells in the spheroids were forming necrotic cores due to the large size of the aggregates.

In summary, liver spheroids, made from HepaRG cells and primary stellate cells, cultured in microfluidic 2-organ chips with or without pancreatic islets were able to display liver-like functions, but were most likely too large to maintain cell viability. PHH spheroids were able to partially predict the metabolism seen in humans *in vivo*, but suffered from decreased metabolic capabilities at the start of the experiment. Further experiments need to be conducted to optimize culturing conditions for both systems in order to establish proper microfluidic co-cultures as well as an improved *in vitro* model for predicting human *in vivo* metabolism.

6. Future studies

In future studies, a complex medium such as the suggested PHH culturing medium for spheroids should be used during MetID experiments. This might improve the metabolic function of the spheroids, possibly allowing for better prediction of human *in vivo* metabolism of compounds. CYP activity of at least the 4 CYPs analyzed in this thesis should be monitored throughout the entire experiment. Suspension cultures using the cells from the same donor and batch should be used as well to eliminate donor variations from the results.

Since the liver is constructed from more cell types than just hepatocytes, incorporating other hepatic cell types into the spheroids will further improve the *in vitro* microenvironment and make it more *in vivo*-like. Incorporation of cells such as Kupffer cells, which are the innate immune cells in the liver, and endothelial cells, which line the sinusoids and biliary ducts in the liver, would be of high interest to examine. Since many metabolites are excreted through the bile in the human liver, epithelial cells might aid in the formation of proper bile canaliculi in the spheroids. Of the same reason, the development of a protocol for establishing bile duct formation and measuring bile excretion is equally important.

The large size of the spheroids used in the chip experiments turned out to be rather disadvantageous. However, handling large quantities of smaller sized spheroids might also produce a large inconvenience. Solutions as to how spheroids might be vascularized, to allow for proper oxygen and nutrient diffusion, should therefore be investigated. Incorporation of endothelial cells into the spheroids, and possibly culturing the cells on a degradable polymeric scaffold, might be a solution. Lastly, co-culturing different types of organ models, such as liver spheroids and pancreatic islets, enables the investigation of organ system functionality. Therefore, by including other organs, such as the kidney or the skin, into the multi-organ chips, other systems and aspects can be examined. For instance, a liver-kidney co-culture could improve the metabolic and excretory predictions of new drugs. Also, including more organs at a time in the microfluidic environment will better simulate the functions of the human body, and can be used to study specific functions in both healthy and diseased models of a human.

Bibliography

[1] J Bailey, M Thew, and M Balls. An analysis of the use of dogs in predicting human toxicology and drug safety. *Alternatives to Laboratory Animals*, 41(5):335–350, 2013.

[2] S. P. S. Monga. *Molecular Pathology of Liver Diseases*. Springer Science + Business Media, New York, 2011.

[3] T. Ohkura, K. Ohta, T. Nagao, K. Kusumoto, A. Koeda, T. Ueda, T. Jomura, T. Ikeya, E. Ozeki, K. Wada, K. Naitoh, Y. Inoue, N. Takahashi, H. Iwai, H. Arakawa, and T. Ogihara. Evaluation of human hepatocytes cultured by three-dimensional spheroid systems for drug metabolism. *Drug metabolism and pharmacokinetics*, 29(5):373–378, 2014.

[4] S Venkatesh and R A Lipper. Role of the development scientist in compound lead selection and optimization. *Journal of pharmaceutical sciences*, 89(2):145–154, 2000.

[5] A Sivaraman, J K Leach, S Townsend, T Iida, B J Hogan, D B Stolz, R Fry, L D Samson, S R Tannenbaum, and L. G Griffith. A microscale *in vitro* physiological model of the liver: predictive screens for drug metabolism and enzyme induction. *Current drug metabolism*, 6(6):569–591, 2005.

[6] K Viravaidya, A Sin, and M L Shuler. Development of a microscale cell culture analog to probe naphthalene toxicity. *Biotechnology progress*, 20(1):316–323, 2004.

[7] D Huh, G A Hamilton, and D E Ingber. From 3D cell culture to organs-on-chips. *Trends in cell biology*, 21(12):745–754, 2011.

[8] C. C. Bell, D. F. Hendriks, S. M. Moro, E. Ellis, J. Walsh, A. Renblom, L. Fredriksson Puigvert, A. C. A. Dankers, F. Jacobs, J. Snoeys, R. L. Sison-Young, R. E. Jenkins, Å. Nordling, S. Mkrtchian, B. K. Park, N. R. Kitteringham, C. E. P. Goldring, V. M. Lauschke, and M Ingelman-Sundberg. Characterization of primary human hepatocyte spheroids as a model system for drug-induced liver injury, liver function and disease. *Nature: Scientific reports*, 6, 2016.

[9] F Pampaloni, E G Reynaud, and E H Stelzer. The third dimension bridges the gap between cell culture and live tissue. *Nature reviews Molecular cell biology*, 8(10):839–845, 2007.

[10] S N Bhatia and D E Ingber. Microfluidic organs-on-chips. *Nature biotechnology*, 32(8):760–772, 2014.

[11] C Zhang, Z Zhao, N A Abdul Rahim, D van Noort, and H Yu. Towards a human-on-chip: culturing multiple cell types on a chip with compartmentalized microenvironments. *Lab on a chip*, 9(22):3185–3192, 2009.

[12] I Wagner, E-M Materne, S Brincker, U Süßbier, C Frädrich, M Busek, F Sonntag, D A Sakharov, E V Trushkin, A G Tonevitsky, R Lauster, and U Marx. A dynamic multi-organ-chip for long-term cultivation and substance testing proven by 3D human liver and skin tissue co-culture. *Lab on a chip*, 13(18):3538–3547, 2013.

[13] I Maschmeyer, T Hasenberg, A Jaenicke, M Lindner, A K Lorenz, J Zech, L-A Garbe, F Sonntag, P Hayden, S Ayehunie, R Lauster, U Marx, and E-M Materne. Chip-based human liver–intestine and liver–skin co-cultures – A first step toward systemic repeated dose substance testing *in vitro*. *European Journal of Pharmaceutics and Biopharmaceutics*, 95:77–87, 2015.

[14] I Maschmeyer, A K Lorenz, K Schimek, T Hasenberg, A P Ramme, J Hübner, M Lindner, C Drewel, S Bauer, A Thomas, N S Sambo, F Sonntag, R Lauster, and U Marx. A four-organ-chip for interconnected long-term co-culture of human intestine, liver, skin and kidney equivalents. *Lab on a Chip*, 15(12):2688–2699, 2015.

[15] E-M Materne, A P Rammea, A P Terrassob, M Serrab, P M Alves, C Brito, D A Sakharov, A G Tonevitsky, R Lauster, and U Marx. A multi-organ chip co-culture of neurospheres and liver equivalents for long-term substance testing. *Journal of biotechnology*, 205:36–46, 2015.

[16] J Iegre, M A Hayes, R A Thompson, L Weidolf, and E M Isin. Database extraction of metabolite information of drug candidates: Analysis of 27 AstraZeneca compounds with human ADME data. *Drug Metabolism and Disposition*, 2016.

[17] J Prieto, J Rodés, and D. A Shafritz. *Hepatobiliary diseases*. Springer-Verlag, Berlin Heidelberg, 1992.

[18] G. J Tortora and B. H Derrickson. *Essentials of anatomy and physiology, 9th ed.* John Wiley & Sons Inc., New York, 2012.

[19] OpenStax CNX. *Accessory Organs in Digestion: The Liver, Pancreas, and Gallbladder*, 2016. `http://cnx.org/contents/FPtK1zmh@6.27:esgfrPlv@3/Accessory-Organs-in-Digestion-` [Accessed: 04-12-2016].

[20] N Katz, H. F Teutsch, K Jungermann, and D Sasse. Heterogenous reciprocal localization of fructose-1, 6-bis-phosphatase and of glucokinase in microdissected periportal and perivenous rat liver tissue. *FEBS letters*, 83(2):272–276, 1977.

[21] S L Friedman. Hepatic stellate cells: protean, multifunctional, and enigmatic cells of the liver. *Physiological reviews*, 88(1):125–172, 2008.

[22] G L Patrick. *An introduction to medicinal chemistry*. Oxford university press, Oxford, 2013.

[23] B Testa and S D Krämer. *The biochemistry of drug metabolism: conjugations, consequences of metabolism, influencing factors*. VHCA/Wiley-VCH, Zürich/Weinheim, 2010.

[24] U. M Zanger and M. Schwab. Cytochrome P450 enzymes in drug metabolism: Regulation of gene expression, enzyme activities, and impact of genetic variation. *Pharmacology & Therapeutics*, 138(1):103–141, 2013.

[25] R Zuber, E Anzenbacherova, and P Anzenbacher. Cytochromes P450 and experimental models of drug metabolism. *Journal of cellular and molecular medicine*, 6(2):189–198, 2002.

[26] A Holstein, A Plaschke, M Ptak, E H Egberts, J El-Din, J Brockmöller, and J Kirchheiner. Association between CYP2C9 slow metabolizer genotypes and severe hypoglycaemia on medication with sulphonylurea hypoglycaemic agents. *British journal of clinical pharmacology*, 60(1):103–106, 2005.

[27] U M Zanger, S Raimundo, and M Eichelbaum. Cytochrome P450 2D6: overview and update on pharmacology, genetics, biochemistry. *Naunyn-Schmiedeberg's archives of pharmacology*, 369(1):23–37, 2004.

[28] R Mannhold, J Kirchmair, and H Kubinyi. *Drug Metabolism Prediction, Volume 63*. Wiley, New York, 2014.

[29] B Prasad, A Garg, H Takwani, and S Singh. Metabolite identification by liquid chromatography-mass spectrometry. *TrAC Trends in Analytical Chemistry*, 30(2):360–387, 2011.

[30] K P Bateman, J Castro-Perez, M Wrona, J P Shockcor, K Yu, R Oballa, and D A Nicoll-Griffith. MSE with mass defect filtering for *in vitro* and *in vivo* metabolite identification. *Rapid communications in mass spectrometry*, 21(9):1485–1496, 2007.

[31] D S Wishart. Advances in metabolite identification. *Bioanalysis*, 3(15):1769–1782, 2011.

[32] N J Clarke, D Rindgen, W A Korfmacher, and K A Cox. Peer reviewed: systematic LC/MS metabolite identification in drug discovery. *Analytical chemistry*, 73(15):430–439, 2001.

[33] Q Cui, I A Lewis, A D Hegeman, M E Anderson, J Li, C F Schulte, W M Westler, H R Eghbalnia, M R Sussman, and J L Markley. Metabolite identification via the madison metabolomics consortium database. *Nature biotechnology*, 26(2):162–164, 2008.

[34] S Moco, J Vervoort, R. J Bino, R. C De Vos, and R Bino. Metabolomics technologies and metabolite identification. *TrAC Trends in Analytical Chemistry*, 26(9):855–866, 2007.

[35] J F Xiao, B Zhou, and H W Ressom. Metabolite identification and quantitation in LC-MS/MS-based metabolomics. *TrAC Trends in Analytical Chemistry*, 32:1–14, 2012.

[36] D C Harris. *Quantitative chemical analysis*. W. H. Freeman and Company, New York, 2010.

[37] B Alberts, A Johnson, J Lewis, M Raff, K Roberts, and P Walter. *Molecular biology of the cell*. Garland science, Taylor & Francis Group, LLC, New York, 2008.

[38] W B Dunn, A Erban, R J Weber, D J Creek, M Brown, R Breitling, T Hankemeier, R Goodacre, S Neumann, J Kopka, and M R Viant. Mass appeal: metabolite identification in mass spectrometry-focused untargeted metabolomics. *Metabolomics*, 9(1):44–66, 2013.

[39] S S Bale, L Vernetti, N Senutovitch, R Jindal, M Hegde, A Gough, W J McCarty, A Bakan, A Bhushan, T Ying Shun, I Bolberg, R DeBiasio, B Osman Usta, D Lansing Taylor, and M L Yarmush. *In vitro* platforms for evaluating liver toxicity. *Experimental biology and medicine*, 239(9):1180–1191, 2014.

[40] E A Blomme, Y Yang, and J F Waring. Use of toxicogenomics to understand mechanisms of drug-induced hepatotoxicity during drug discovery and development. *Toxicology letters*, 186(1):22–31, 2009.

[41] V Y Soldatow, E L LeCluyse, L G Griffith, and I Rusyn. *In vitro* models for liver toxicity testing. *Toxicology research*, 2(1):23–39, 2013.

[42] A Damania, E Jain, and A Kumar. Advancements in *in vitro* hepatic models: application for drug screening and therapeutics. *Hepatology international*, 8(1):23–38, 2014.

[43] K-S Vellonen, M Malinen, E Mannermaa, A Subrizi, E Toropainen, Y-R Lou, H Kidron, M Yliperttula, and A Urtti. A critical assessment of in vitro tissue models for ADME and drug delivery. *Journal of Controlled Release*, 190:94–114, 2014.

[44] T B Andersson, K P Kanebratt, and J G Kenna. The HepaRG cell line: a unique *in vitro* tool for understanding drug metabolism and toxicology in human. *Expert opinion on drug metabolism & toxicology*, 8(7):909–920, 2012.

[45] K. P. Kanebratt and T. B. Andersson. Evaluation of HepaRG cells as an *in vitro* model for human drug metabolism studies. *Drug metabolism and disposition*, 36(7):1444–1452, 2008.

[46] S F Abu-Absi, L K Hansen, and W S Hu. Three-dimensional co-culture of hepatocytes and stellate cells. *Cytotechnology*, 45(3):125–140, 2004.

[47] R J Thomas, R Bhandari, D A Barrett, A J Bennett, J R Fry, D Powe, B J Thomson, and K M Shakesheff. The effect of three-dimensional co-culture of hepatocytes and hepatic stellate cells on key hepatocyte functions *in vitro*. *Cells Tissues Organs*, 181(2):67–79, 2005.

[48] D Huh, Y S Torisawa, G A Hamilton, H J Kim, and D E Ingber. Microengineered physiological biomimicry: organs-on-chips. *Lab on a chip*, 12(12):2156–2164, 2012.

[49] N J Douville, Y C Tung, R Li, J D Wang, M E El-Sayed, and S Takayama. Fabrication of two-layered channel system with embedded electrodes to measure resistance across epithelial and endothelial barriers. *Analytical chemistry*, 82(6):2505–2511, 2010.

[50] M C Liu, H C Shih, J G Wu, T W Weng, C Y Wu, J C Lu, and Y C Tung. Electrofluidic pressure sensor embedded microfluidic device: a study of endothelial cells under hydrostatic pressure and shear stress combinations. *Lab on a Chip*, 13(9):1743–1753, 2013.

[51] T A Nguyen, T I Yin, D Reyes, and G A Urban. Microfluidic chip with integrated electrical cell-impedance sensing for monitoring single cancer cell migration in three-dimensional matrixes. *Analytical chemistry*, 85(22):11068–11076, 2013.

[52] D Huh, B D Matthews, A Mammoto, M Montoya-Zavala, H Y Hsin, and D E Ingber. Reconstituting organ-level lung functions on a chip. *Science*, 328(5986):1662–1668, 2010.

[53] J W Allen and S N Bhatia. *In vitro* zonation and toxicity in a hepatocyte bioreactor. *Toxicological sciences*, 84(1):110–119, 2005.

[54] J W Allen, S R Khetani, and S N Bhatia. Formation of steady-state oxygen gradients *in vitro*: Application to liver zonation. *Biotechnology and bioengineering*, 82(3):253–262, 2003.

[55] A Carraro, W M Hsu, K M Kulig, W S Cheung, M L Miller, E J Weinberg, E F Swart, M Kaazempur-Mofrad, J T Borenstein, J P Vacanti, and C Neville. *In vitro* analysis of a hepatic device with intrinsic microvascular-based channels. *Biomedical microdevices*, 10(6):795–805, 2008.

[56] P Chao, T Maguire, E Novik, K C Cheng, and M L Yarmush. Evaluation of a microfluidic based cell culture platform with primary human hepatocytes for the prediction of hepatic clearance in human. *Biochemical pharmacology*, 78(6):625–632, 2009.

[57] S Cheng, J M Prot, E LeClerc, and F Y Bois. Zonation related function and ubiquitination regulation in human hepatocellular carcinoma cells in dynamic vs. static culture conditions. *BMC genomics*, 13(1):54, 2012.

[58] B J Kane, M J Zinner, M L Yarmush, and M Toner. Liver-specific functional studies in a microfluidic array of primary mammalian hepatocytes. *Analytical Chemistry*, 78(13):4291–4298, 2006.

[59] P J Lee, P J Hung, and L P Lee. An artificial liver sinusoid with a microfluidic endothelial-like barrier for primary hepatocyte culture. *Biotechnology and bioengineering*, 97(5):1340–1346, 2007.

[60] S A Lee, E Kang, J Ju, D S Kim, and S H Lee. Spheroid-based three-dimensional liver-on-a-chip to investigate hepatocyte-hepatic stellate cell interactions and flow effects. *Lab on a Chip*, 13(18):3529–3637, 2013.

[61] A Legendre, R Baudoin, G Alberto, P Paullier, M Naudot, T Bricks, J Brocheton, S Jacques, J Cotton, and E Leclerc. Metabolic characterization of primary rat hepatocytes cultivated in parallel microfluidic biochips. *Journal of pharmaceutical sciences*, 102(9):3264–3276, 2013.

[62] Y Nakao, H Kimura, Y Sakai, and T Fujii. Bile canaliculi formation by aligning rat primary hepatocytes in a microfluidic device. *Biomicrofluidics*, 5(2), 2011.

[63] E Novik, T J Maguire, P Chao, K C Cheng, and M L Yarmush. A microfluidic hepatic coculture platform for cell-based drug metabolism studies. *Biochemical pharmacology*, 79(7):1036–1044, 2010.

[64] M J Powers, K Domansky, M R Kaazempur-Mofrad, A Kalezi, A Capitano, A Upadhyaya, P Kurzawski, K E Wack, D Beer Stolz, R Kamm, and L G Griffith. A microfabricated array bioreactor for perfused 3D liver culture. *Biotechnology and Bioengineering*, 78(3):257–269, 2002.

[65] M J Powers, D M Janigian, K E Wack, C S Baker, D B Stolz, and L G Griffith. Functional behavior of primary rat liver cells in a three-dimensional perfused microarray bioreactor. *Tissue engineering*, 8(3):499–513, 2002.

[66] A Sin, K C Chin, M F Jamil, Y Kostov, G Rao, and M Shuler. The design and fabrication of three-chamber microscale cell culture analog devices with integrated dissolved oxygen sensors. *Biotechnology progress*, 20(1):338–345, 2004.

[67] Y C Toh, T C Lim, D Tai, G Xiao, D van Noort, and H Yu. A microfluidic 3D hepatocyte chip for drug toxicity testing. *Lab on a Chip*, 9(14):2026–2035, 2009.

[68] K Viravaidya and M L Shuler. Incorporation of 3T3-L1 cells to mimic bioaccumulation in a microscale cell culture analog device for toxicity studies. *Biotechnology progress*, 20(2):590–597, 2004.

[69] A K H Achyuta, A J Conway, R B Crouse, E C Bannister, R N Lee, C P Katnik, A A Behensky, J Cuevas, and S S Sundaram. A modular approach to create a neurovascular unit-on-a-chip. *Lab on a Chip*, 13(4):542–553, 2013.

[70] K J Jang, A P Mehr, G A Hamilton, L A McPartlin, S Chung, K Y Suh, and D E Ingber. Human kidney proximal tubule-on-a-chip for drug transport and nephrotoxicity assessment. *Integrative Biology*, 5(9):1119–1129, 2013.

[71] L Schäffer, C L Brand, B F Hansen, U Ribel, A C Shaw, R Slaaby, and J Sturis. A novel high-affinity peptide antagonist to the insulin receptor. *Biochemical and biophysical research communications*, 376(2):380–383, 2008.

[72] W Tang. The metabolism of diclofenac-enzymology and toxicology perspectives. *Current drug metabolism*, 4(4):319–329, 2003.

[73] M. Darnell, M. Ulvestad, E. Ellis, L. Weidolf, and T. B. Andersson. In vitro evaluation of major in vivo drug metabolic pathways using primary human hepatocytes and heparg cells in suspension

and a dynamic three-dimensional bioreactor system. *Journal of Pharmacology and Experimental Therapeutics*, 343(1):134–144, 2012.

[74] S Kidambi, R S Yarmush, E Novik, P Chao, M L Yarmush, and Y Nahmias. Oxygen-mediated enhancement pf primary hepatocyte metabolism, functional polarization, gene expression, and drug clearance. *Proceedings of the National Academy of Sciences*, 106(37):15714–15719, 2009.

[75] H Girgis, O Masui, N M White, A Scorilas, F Rotondo, A Seivwright, M Gabril, E R Filter, A H A Girgis, G A Bjarnason, M A S Jewett, A Evans, S Al-Haddad, K W M Siu, and G M Yousef. Hepatic stellate cells: protean, multifunctional, and enigmatic cells of the liver. *Lactate dehydrogenase A is a potential prognostic marker in clear cell renal cell carcinoma*, 13(1):101, 2014.

[76] M Lübberstedt, U Müller-Vieira, M Mayer, K M Biemel, F Knöspel, D Knobeloch, A K Nüssler, J C Gerlach, and K Zeilinger. HepaRG human hepatic cell line utility as a surrogate for primary human hepatocytes in drug metabolism assessment in vitro. *Journal of pharmacological and toxicological methods*, 63(1):59–68, 2011.

[77] E Curcio, S Salerno, G Barbieri, L De Bartolo, E Drioli, and A Bader. Mass transfer and metabolic reactions in hepatocyte spheroids cultured in rotating wall gas-permeable membrane system. *Biomaterials*, 28(36):5487–5497, 2007.

[78] R Z Lin and H Y Chang. Recent advances in three-dimensional multicellular spheroid culture for biomedical research. *Biotechnology journal*, 3(9-10):1172–1184, 2008.

[79] I Quesada, E Tudurí, C Ripoll, and Á Nadal. Physiology of the pancreatic α-cell and glucagon secretion: role in glucose homeostasis and diabetes. *Journal of Endocrinology*, 199(1):5–19, 2008.